NASA TT F-9142

SPECTRAL DISTRIBUTION OF DIRECT AND DIFFUSE SOLAR RADIATION

O. Avaste, Kh. Moldau, K. S. Shifrin

Translation of "Spektral'noye raspredeleniye pryamoy
i rasseyannoy radiatsii."
Akademiya Nauk ESSR, Institut Fiziki i Astronomii
Issledovaniya po Fizike Atmosfery
Vol. 3, pp. 23-70, 1962.

(Latvian)

OTS PRICE

XEROX $ 2.00 FS

MICROFILM $ .50 MF

FACILITY FORM 602

N65 11694 (ACCESSION NUMBER)

46 (PAGES)

(NASA CR OR TMX OR AD NUMBER)

(THRU)

1 (CODE)

29 (CATEGORY)

NATIONAL AERONAUTICS AND SPACE ADMINISTRATION
WASHINGTON OCTOBER 1964

SPECTRAL DISTRIBUTION OF DIRECT AND DIFFUSE SOLAR RADIATION

/23

O. Avaste, Kh. Moldau, K. S. Shifrin[1]

11694

ABSTRACT

The results of the calculations of the spectral distribution of direct and scattered solar radiation under various degrees of atmospheric clarity are given with consideration for the absorption of body water vapor, carbon dioxide, and ozone. The calculations for the Standard Radiation Model of the atmosphere coincide quite well with the mean experimental data. An approximation formula is proposed for determining the albedo effect on the descending scattered radiation flux for the cases of real absorption. It also shows that the real observation of the elongation of the atmospheric indicatrix of scattering with the increase in the wavelength directly follows the scheme of K. S. Shifrin and I. N. Minin.

Author

Introduction

This study gives the results of the calculations of the spectral fluxes of direct and scattered radiation according to the method given in Reference 1. The plane-parallel model of real atmosphere has been considered.

Changes in the spectral composition of the solar radiation in the atmosphere depend primarily on two factors: (1) molecular scattering, most intensive in the short wavelength range, and (2) selective absorption by the water vapor in the near infrared spectrum region. Aside from this, scattering on the aerosol and absorption by ozone, carbon dioxide and the permanent components of the atmosphere are also important. The spectral distribution of the solar radiations outside the atmosphere was taken from Johnson (Ref. 2).

/24

The concentration of water vapor decreases exponentially with the height (after Yamamoto formula; Ref. 3), the volume concentration of carbon dioxide is constant (0.033 percent), and virtual temperature

---

[1] K. S. Shifrin (Main Geophysical Observatory named after A. I. Voyeykov, Leningrad).

diminishes linearly with height. The weakening of aerosol and molecular densities was calculated according to the scheme of K. S. Shifrin and I. N. Minin (Ref. 4). Absorption by the ozone is considered by the introduction of a "subozone" spectral density of the direct solar radiation (same as in Refs. 5 and 6). In the first approximation, the absorption coefficient of ozone can be considered as independent of the quantity of the ozone encountered by the ray. The mean absorption coefficient of ozone in the spectral regions was found in the data of I. A. Prokof'yeva (Ref. 7). The general content of ozone in the atmosphere is taken as being equal to 0.25 atm·cm (thickness of the equivalent layer of ozone in centimeters at normal pressure and temperature). The model used here is described in greater detail in Reference 1. The absorption of radiation by water vapors and carbon dioxide was considered by using the mean absorption functions in lines, obtained from the experimental data of Howard, Burch, and Williams (Ref. 8). For the line 0.7 μ-Φ, the data used was obtained by Fowle (Ref. 9). The effect of pressure on absorption is also considered (see Ref. 1).

Calculations of the Direct Solar Radiation

The intensity of direct radiation in the given spectral interval is obtained by using the formula:

$$I_\lambda(z, m) = I_{0,\lambda} e^{-m[\tau_z^\infty(\lambda)+k_\lambda\omega]} T(x_w\sqrt{m})\, T(\bar{x}_{CO_2}\sqrt{m}), \qquad (1)$$

where m is the atmospheric mass (from tables by Bemporad), z is the height above the surface of the earth, k_λ is the absorption coefficient of ozone, ω is the ozone content in atm·cm, $\tau_z^\infty(\lambda)$ is the optical thickness of the atmosphere from the z level to the upper boundary of the atmosphere (for the center of the given spectral interval), $I_{0,\lambda}$ is part of the direct solar radiation beyond the atmosphere descending upon the given spectral interval, $T(\bar{x}_w\sqrt{m})$ and $T(\bar{x}_{CO_2}\sqrt{m})$ are in accordance with the penetrability function of water vapor and carbon dioxide (after study; Ref. 1). In (1), the absorption of the permanent gases of the atmosphere was not taken into consideration. This means that it is correct with the exception of two small regions near the oxygen lines 0.69 μ and 0.76 μ.

/25

The integral flux of direct solar radiation is expressed by:

$$S(z, m) = \int_0^\infty I_{0,\lambda} e^{-m[\tau_z^\infty(\lambda)+k_\lambda\omega]} T(\bar{x}_w\sqrt{m}) T(\bar{x}_{CO_2}\sqrt{m})\, d\lambda - \left| - f_3(m) \frac{S(z, m)}{S_{id}(z, m)} \right| \quad (2)$$

where $f_3(m)$ is the correction for the absorption by the permanent gases in the ideal, pure air, dry atmosphere after Kastrov (Ref. 10), and $S_{id}(z, m)$ is the integral flux of direct solar radiation in pure and dry atmosphere with atmospheric mass m at height z from the surface of the earth.

The results of the calculations are given in the supplementary tables which also give data on the energy of the corresponding spectral intervals in mcal/cm^2·min.[1] From Figure 1 we obtain the general idea about the changes of the spectral intensity of the direct solar radiation in cal/cm^2·min·μ in real atmosphere on the earth's surface with m = 2. This gives the intensities at mean optical condition of the atmosphere ($\tau_0(\lambda_0)$ = 0.3, λ_0 = 0.550 μ, w = 2.1 cm), weak murky atmosphere ($\tau_0(\lambda_0)$ = 0.2, w = 0.5 cm) and ($\tau_0(\lambda_0)$ = 0.5, w = 3.0 cm) highly murky atmosphere. /26

Table 1 of the supplement gives the so-called subozone distribution of energy in the spectrum of direct solar radiation. Table 2 of the supplement gives the spectral distribution of the direct solar radiation at the earth's surface at different degrees of murkiness and water vapor content. Table 3 of the supplement gives the spectral distribution of the energy of direct solar radiation at different heights for the mean standard radiation model of the atmosphere ($\tau_0(\lambda_0)$= 0.3, w = 2.1 cm).

We should like to note that the spectral intensity of direct solar radiation, calculated after Table 3 of the supplement, at the height of z = 20 km, coincides, for m = 1 to 4 with an accuracy to 1 percent, with values calculated by using the data of L. A. Biryukova (Ref. 11). In comparing the spectral intensities at a height of 9 km with the data in Reference 11 at a height of 10 km, we see that when m = 1, our data is less accurate by 1-2 percent, and when m = 4, it is less accurate by 6-8 percent. Apparently, this is because the calculations of Biryukova were made for an ideal atmosphere, whereas in our model of the atmosphere, the aerosol was distributed up to 11 km high. /27

[1] mcal = 10^{-3} cal.

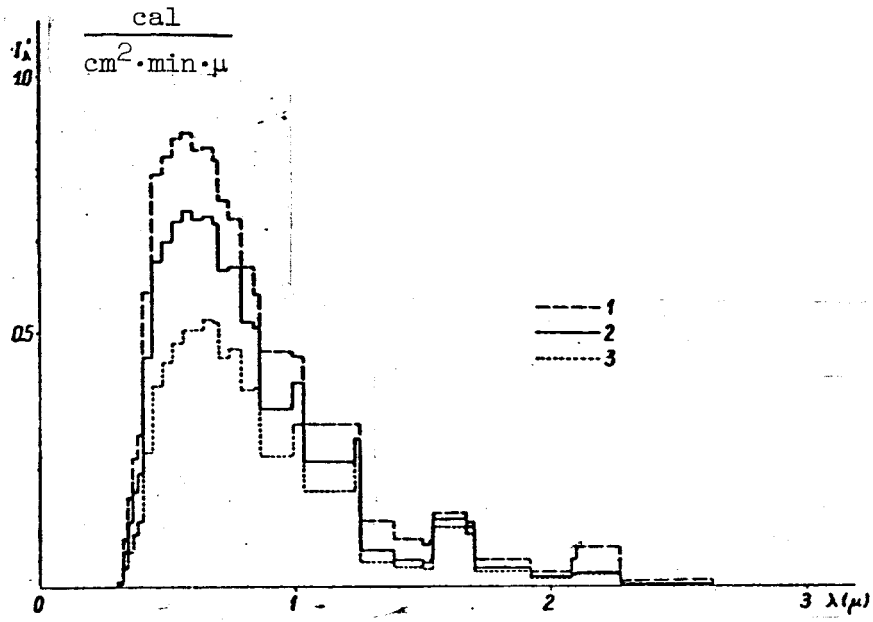

Figure 1. Spectral distribution of direct solar radiation on the horizontal surface when m = 2 on the earth's surface. 1, $\tau_0(\lambda_0)$ = 0.2, w = 0.5 cm; 2, $\tau_0(\lambda_0)$ = 0.3, w = 2.1 cm; 3, $\tau_0(\lambda_0)$ = 0.5, w = 3.0 cm

Calculations of the Scatter Radiation Outside the Lines of Absorption

For calculating the descending spectral fluxes of the scattering radiation at the earth's surface outside the lines of absorption, we have used the formula from the V. V. Sobolev method of approximation (Ref. 12):

$$F_{D,\lambda} = \frac{2\pi R(\tau_{0,\lambda}, i)\cos i}{4 + (1 - A_\lambda)(3 - \varkappa_1)\tau_{0,\lambda}} - \pi e^{-\tau_{0,\lambda}\sec i} \cos i. \quad (3)$$

where i is the azimuth angle of the sun, $\tau_{0,\lambda}$ is the spectral optical thickness of the atmosphere, and A_λ is the spectral albedo of the sub-layer surface. The function $R(\tau_{0,\lambda}, i)$ was determined by the expression:

$$R(\tau_{0,\lambda}, i) = 1 + \frac{3}{2}\cos i + \left(1 - \frac{3}{2}\cos i\right) e^{-\tau_{0,\lambda}\sec i}, \quad (4)$$

Table 1. Descending Fluxes of the Scatter Radiation F_D on the Surface of the Earth, Calculated by the V. V. Sobolev Method (S) and by the Method of Successive Approximation (IFA) (Ref. 15) and When Albedo A = 0

τ_0	No. of indicatrix	F_D(IFA)				F_D(S)				F_D(S)/F (IFA)			
		30	45	60	75	30	45	60	75	30	45	60	75
0.2	V	0.3157	0.3022	0.2685	(0.1165)	0.348	0.326	0.294	0.219	1.10	1.08	1.09	1.88
	VI	0.3450	0.3279	0.2869	(0.1212)	0.377	0.350	0.309	0.226	1.09	1.07	1.08	1.86
0.4	VI	0.6036	0.5464	0.4468	0.2818	0.656	0.596	0.501	0.336	1.09	1.09	1.12	1.19
	VII	0.6919	0.6188	0.4944	0.2986	0.737	0.659	0.542	0.354	1.06	1.07	1.10	1.18
0.6	VII	0.9002	(0.7236)	0.5833	0.3075	0.964	0.847	0.667	0.388	1.07	1.17	1.14	1.26
	VIII	0.9956	0.8566	0.6278	0.3326	1.046	0.910	0.707	0.404	1.05	1.06	1.13	1.22
0.8	VII	1.0378	0.8718	(0.5362)	0.2828	1.128	0.971	0.736	0.390	1.09	1.11	1.37	1.38
	VIII	1.1492	0.9534	0.6549	0.2938	1.226	1.046	0.782	0.409	1.07	1.10	1.19	1.39

and the constant $\varkappa_1$, characterizing the elongation of scatter indicatrix, was determined by:

$$\varkappa_1 = \frac{3}{2}\int_0^{\pi} \varkappa(\gamma) \sin\gamma \cos\gamma d\gamma, \tag{5}$$

where $\varkappa(\gamma)$ is the scatter indicatrix and γ is the angle of scatter.

As References 13 and 14 show, in the calculations of the descending intensities for the elongated scattering indicatrix by the V. V. Sobolev method of approximation the errors around the 90° angle of scattering reach a considerably large quantity. Let us explain the degree of precision of (3) in anisotropic scattering. For this purpose let us solve the problem for the double layer model of the atmosphere and compare this solution with the numerical solution obtained at IFA (Table IV in Ref. 15). The results are given in Table 1. /29

The values of the fluxes in Table 1 and in (3) are expressed in the relative units (twice larger than in Ref. 15). If the solar constant in this given segment of the spectra is taken as being equal to $I_{0,\lambda}$ cal/cm^2·min·μ, then the absolute value of the fluxes can be obtained by multiplying the data given in the tables by $I_{0,\lambda}/\pi$. The calculations were conducted with albedo A = 0, of the double layer model of the atmosphere while for the upper layer $\tau_1 = 1/4\ \tau_0$ I indicatrix after Foitzik and Zchaeck in (Ref. 16) was taken. The numbers of the indicatrix of the lower layer are given in the second column of Table 1. The formulas for calculating the double layer model of the atmosphere by the Sobolev method are given in Reference 17.

From Table 1 we can see that the errors in calculating the descending flux of the scattering radiation increases with the increase of the sun's azimuth angle. In Table 1, we linearly extrapolated the values for errors obtained in F_D for the great optical thicknesses. The results are given in Figure 2. In Table 1, four values in the IFA calculations are given in parentheses. These values are probably minimized, since in this case the relationships $F_D(C)/F_D$ (IFA) are extremely large.

As an example, we use the calculations of the descending flux of the scatter of radiation in general standard optical conditions of the atmosphere ($\tau_0(\lambda_0) = 0.3$, w = 2.1 cm) with the atmospheric mass m = 2.

The results are given in Table 4 of the supplement. The spectral albedo of the surface of the earth were taken from the study by Dirmhirn (Ref. 18). To take into consideration the weakening caused by ozone, instead of the spectral solar constant we used the meaning subozone solar radiation, i.e., the absolute values of the fluxes obtained by multiplying /30

by $\frac{I_{0,\lambda}e^{-k_\lambda \omega m}}{\pi}$ the quantities calculated using formula (3) (see supplementary Table 1).

Figure 3 gives the result of the calculations of the scattered radiation during summer when m = 2. The dashed line represents calculations made by using (3), the solid line represents the corrected data, in which the dependence of the errors on the optical thickness (see Figure 2) was taken into consideration. In the near infrared region in the absorption line, the scattered radiation fluxes were calculated with the consideration of singular scattering and absorption.

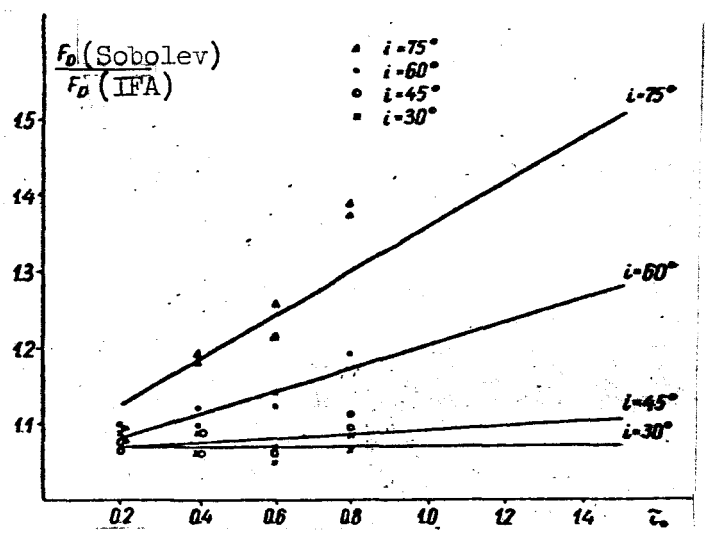

Figure 2. The relationship of the descending fluxes of the scattered radiation calculated by the V. V. Sobolev method (S), and the values of the fluxes calculated by the successive approximation method (IFA), and their dependence on the optical thickness τ_0 and the azimuth angle of the sun i

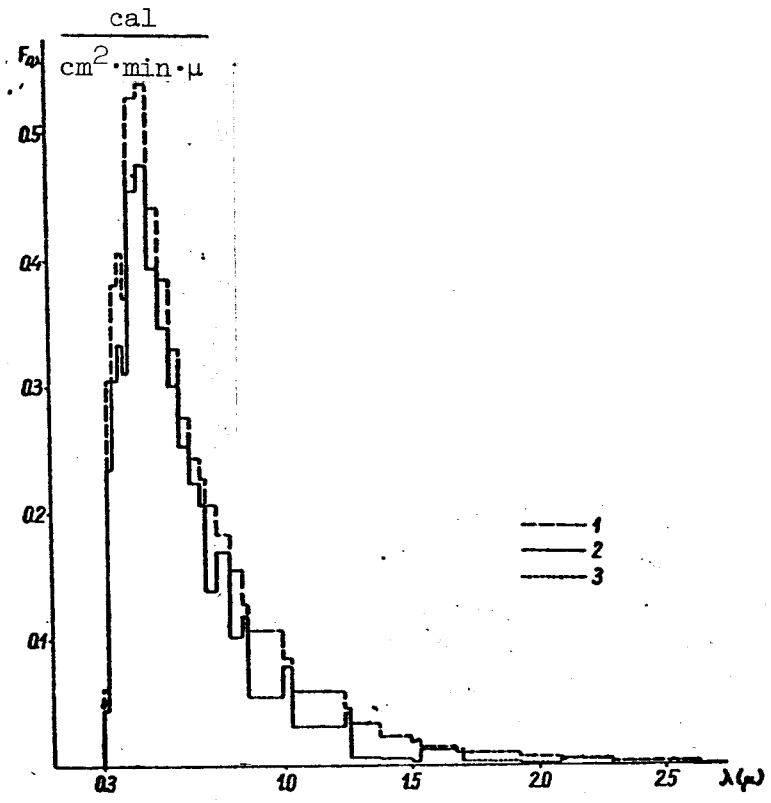

/31

Figure 3. The spectral distribution of the scattering radiation flux on the surface of the earth when m = 2, $\tau_0(\lambda_0) = 0.3$, $\omega = 2.1$ cm. 1, calculated using formula (3); 2, considering the corrections given in Figure 2; 3, considering the absorption in the lines of the water vapor and carbon dioxide

Calculations of the Scattering Radiation with the Consideration of True Absorption

In the case of the true absorption and when the albedo is different from 0, instead of (3), we obtain an approximation formula:

$$F_{D,\lambda}(\tilde{\lambda}, A_\lambda) = F^0_{D,\lambda} + (F^0_{D,\lambda} + I_\lambda') \frac{\tilde{\lambda} A_\lambda}{\frac{4}{a\tau_{0,\lambda}} + 1 - A_\lambda}, \qquad (6)$$

/32

where,

$$a = 3 - \varkappa_1, \qquad (7)$$

$$I_\lambda' = \pi e^{-\tau_\lambda m} T(\bar{x}_w \sqrt{m}) T(\bar{x}_{CO_2} \sqrt{m}) \cos i \tag{8}$$

is the monochromatic flux of direct solar radiation on the horizontal surface, $F^0_{D,\lambda}$--monochromatic flux of the descending scatter radiation on the surface of the earth when albedo A = 0. In (6), the quantity $\bar{\lambda}$, characteristic of the absorption, is determined by the following method:

$$\bar{\lambda} = \frac{\tau_\lambda(\sigma_\lambda, \overline{\sec \vartheta})}{\tau_\lambda(\sigma_\lambda, \overline{\sec \vartheta}) + \tau_\lambda(k_\lambda, \overline{\sec \vartheta})}, \tag{9}$$

where,

$$\tau_\lambda(\sigma_\lambda, \overline{\sec \vartheta}) = \overline{\sec \vartheta} \int_0^\infty \sigma_\lambda \, dz \tag{10}$$

is the optical thickness of the scattering atmosphere in the direction $\vartheta = \text{arc } \overline{\sec \vartheta}$, $\overline{\sec \vartheta} = 1.66$. Since τ_λ (σ_λ, $\overline{\sec \vartheta}$) when the changes in the wavelength are small, its change is also insignificant, so that we can use its mean value for the spectral regions given in the supplement. The value τ_λ (k_λ, $\overline{\sec \vartheta}$) is the optical thickness of the absorbing atmosphere in the direction $\vartheta = \text{arc } \overline{\sec \vartheta}$, $\overline{\sec \vartheta} = 1.66$. Taking into consideration that the absorption in the near infrared region of the spectrum is highly selective, we shall attempt to tie the quantity v_λ (k_λ, $\overline{\sec \vartheta}$) with the mean filtration function in the absorption lines $T(x_w \sqrt{\overline{\sec \vartheta}})$.

The weakening of the monochromatic radiation can be described by the Lambert-Bouguer law:

$$dI_\lambda = -k_\lambda I_\lambda dz. \tag{11}$$

By using the filtration function, the weakened radiation can be represented by: /33

$$I(\bar{x}_w) = I_0 T(\bar{x}_w). \tag{12}$$

and from here,

$$d \ln I = d \ln [T(\bar{x}_w)] \tag{13}$$

and by considering (11) and (13), we obtain:

$$\tau_\lambda(k_\lambda) = \int_0^z k_\lambda dz = -\int_0^z \frac{dI}{I} = -\ln[T(\bar{x}_w)]. \tag{14}$$

Then for the parameter $\tilde{\lambda}$, we obtain the formula:

$$\tilde{\lambda} = \frac{\tau_\lambda(\sigma_\lambda, \overline{\sec\vartheta})}{\tau_\lambda(\sigma_\lambda, \overline{\sec\vartheta}) - \ln[T(\bar{x}_w \sqrt{\overline{\sec\vartheta}})]}. \tag{15}$$

The spectrofluxes in the absorption lines of Figure 3 (dotted lines) were calculated by using (6), where $F^0_{D,\lambda}$ were calculated by the method in Ref. 1 and considered the singular scattering and absorption.

It should be noted that if we calculate the spectrofluxes of the scattering radiation, considering only singular scattering outside the absorption lines near the infrared region, then we will obtain values which will be between 10-12 percent below the values calculated by using (3), with the considerations of the corrections in Figure 2. If the multiple scattering in the absorption lines is not considered, then obviously this will result only in a very insignificant error.

The calculated integral fluxes of the scattered radiation (see supplementary Table 4) are very close to the measured values for the scattered radiation at Tartu (Ref. 19): when m = 2, F_D = 90-200 mcal/cm^2·min during the summer, and F_D = 140-230 mcal/cm^2·min during the winter.

In Table 4 of the supplement, we can see that the integral fluxes of the spectral region 0.7-4.0 μ during winter and summer differ very little. The growth of the integral flux (0.29-4.0 μ) of the scattered radiation during winter, as compared with summer (at exactly the same altitude of the sun and the degree of murkiness of the atmosphere), is explained by the greater values of the albedo during winter in the visual range of the spectrum. /35

In Table 5 of the supplement are given relative distributions of the spectral regions of direct solar radiation (m = 1.5, 2, 4) and scattering radiation when m = 2 during winter and summer for the standard radiation model of the atmosphere. Figure 4 gives the comparison of the spectra of direct solar and scattered radiation of the various authors in the study by Yu. D. Yanishefskiy (Ref. 20) and the curves calculated by us. Probably the distribution of radiation in Reference 20 is exaggerated in the ultraviolet region of the spectrum. Aside from this, our curve shows the effect of the absorption in the lines of the water vapor. /36

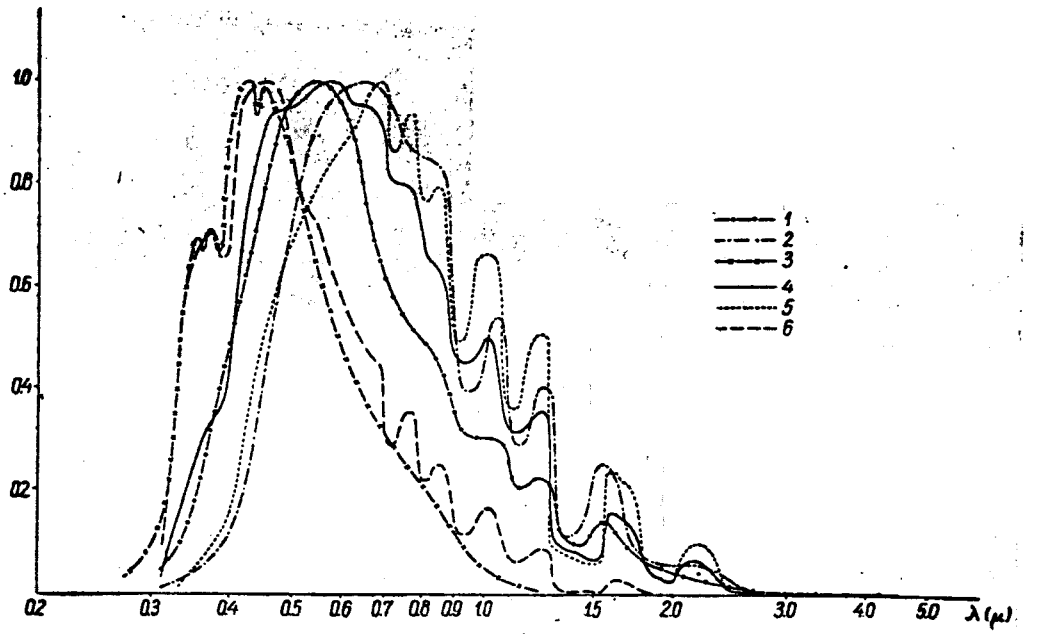

Figure 4. The spectral distribution of direct solar radiation I_λ in various masses of the atmosphere and scattered radiation of the cloudless sky $F_{D,\lambda}$ during summer, in study (Ref. 20), and calculated by us. 1, I_λ (m = 1.4) in study (Ref. 20); 2, I_λ (m = 4) in study (Ref. 20); 3, $F_{D,\lambda}$ (m = 2.45) in study (Ref. 20); 4, I_λ (m = 1.5) calculated; 5, I_λ (m = 4) calculated; 6, $F_{D,\lambda}$ (m = 2) calculated

Table 6 in the supplement gives relative distribution along the spectral regions of the direct solar and scattered radiation when m = 2, w = 2.1 cm, $\tau_0(\lambda_0) = 0.3$. The values in Table 5 of the supplement are normative in accordance with the maxima, and the values in Table 6 of the supplement are normative according to the integral fluxes.

Table 7 of the supplement gives relative spectral intensities of the descending scattering radiation in the near infrared region of the spectrum when $\tau_0(\lambda_0) = 0.3$ and w = 2.1 cm, for m = 2 and m = 6 on the surface of the earth, and for m = 2 at the height of z = 3 km. The /37

table also gives the intensities in the azimuth in mcal/cm^2·min·μ. The calculations were made according to the method given in Reference 1 for the standard radiation model of the atmosphere. The mean indicatrix of scattering $\overline{\varkappa_{VII}(\gamma)}$ is given in Reference 1 (Table 10). The elongation of the indicatrix is characterized by the parameter $\varkappa_1 = 0.967$: see formula (5). The dependence of the intensity of the scattered radiation on the direction can be best represented on the isophoto maps. In Figures 5-10, the solid line shows isophotos outside the spectrum of absorption, while the dotted lines are in the absorption spectrum of the weak line 0.8 μ and the strong line ψ.

The Dependence of the Scattering Indicatrix on the Wavelength /39

It should be pointed out that the calculations of the distribution of the spectral intensity were done when albedo A = 0 and the scattering indicatrix $\overline{\varkappa_{VII}(\gamma)}$ (see Ref. 1). Some literature points out that in

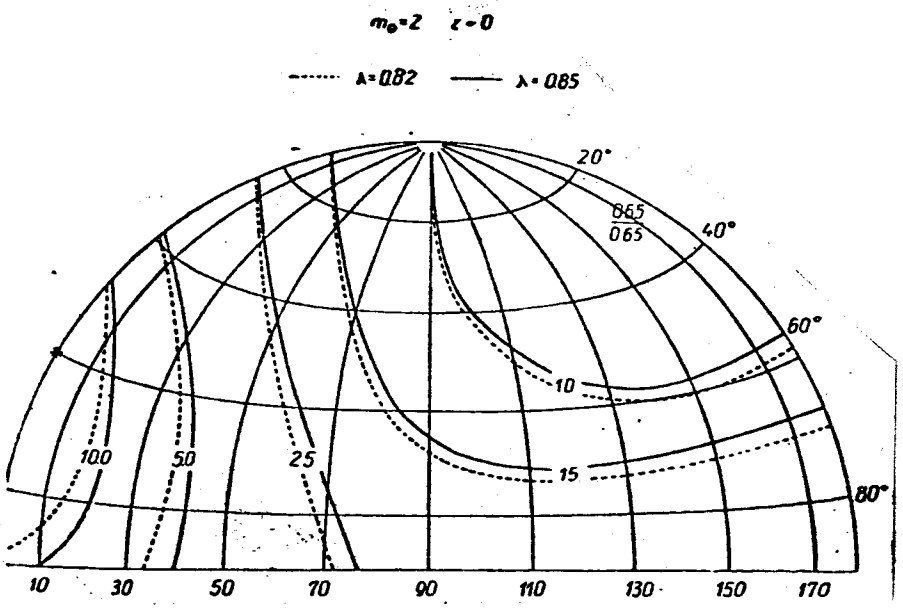

Figure 5. Isophotos of the scatter radiation in the absorption spectrum 0.8 μ and outside the spectrum when m = 2, z = 0. Numbers around the 90° angle of scattering show correspondingly the values of the minima outside the absorption line (numerator) and in the absorption line (denominator)

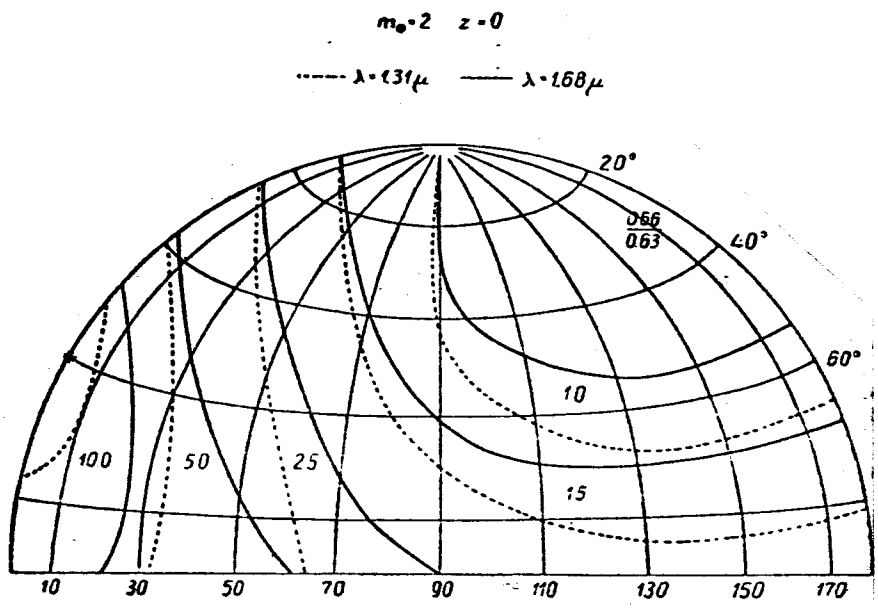

Figure 6. Isophotos of the scattering radiation in the absorption line ψ and outside the line when m = 2, z = 0

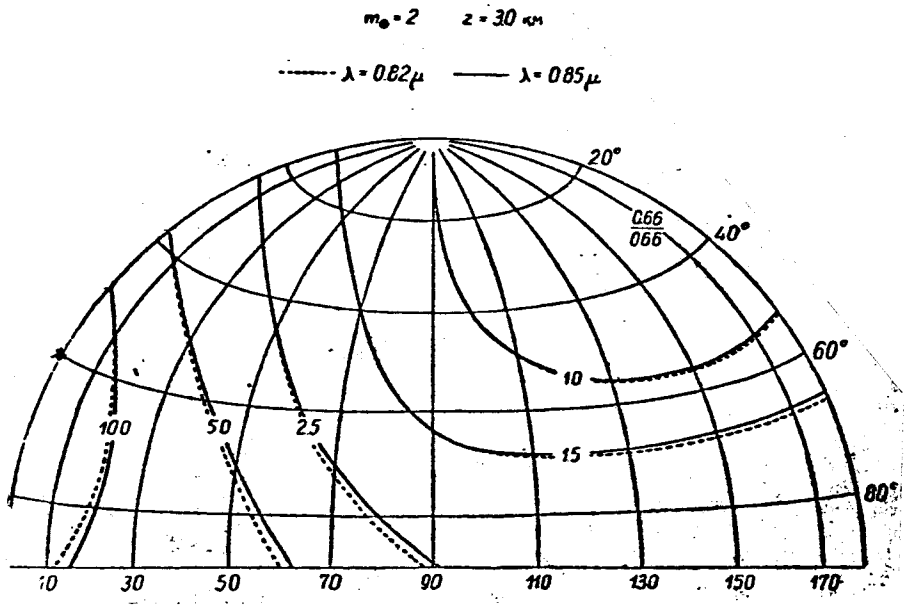

Figure 7. Isophotos of the scattered radiation in the absorption spectrum 0.8 μ and outside the spectrum when m = 2, z = 3.0 km

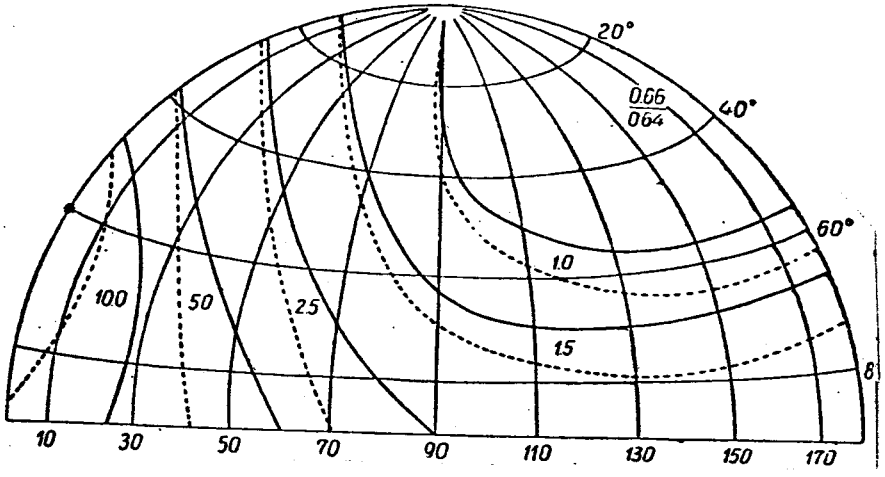

Figure 8. Isophotos of scattered radiation in the absorption spectrum ψ and outside the spectrum when m = 2, z = 3.0 km (m⊙ = 2, z = 30 km ..... λ = 1.31 μ; _____ λ = 1.68 μ)

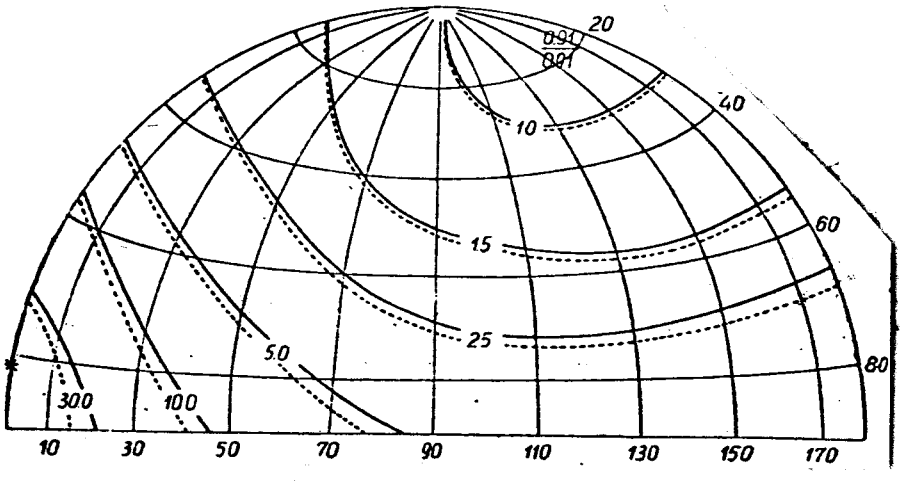

Figure 9. Isophotos of the scattered radiation in the absorption spectrum 0.8 μ and outside the spectrum when m = 6, z = 0 km (m⊙ = 6, z = 0; ..... λ = 0.82 μ, _____ λ = 0.85 μ)

the near infrared region, the intensity has a strong forward scattering as compared with the visible spectrum (Refs. 21-24). This means that in the near infrared region the real indicatrices are more elongated than they are in the visible region of the spectrum.

The comparison of the calculated intensities in the absorption spectrum with the experimental intensities (Ref. 25), shows that the intensity of the azimuth is of the same order, but the minimum around the scattering angle $\gamma = 90^\circ$ obtained from the experimental data is much deeper. This is in accordance with the fact that the indicatrices in /40

the near infrared region are more elongated than $\overline{\varkappa_{VII}(\gamma)}$ which we used.

It should be noted that the elongation of the atmospheric indicatrix with the increase of the wavelength stems directly from the scheme of K. S. Shifrin and I. N. Minin (Ref. 4). Let us consider the formula for the mean atmospheric indicatrix they proposed (formula (38) in Ref. 4):

$$\varkappa(\gamma) = \frac{p}{\tau_0}\varkappa_p(\gamma) + \frac{q}{\tau_0}\varkappa_a(\gamma), \tag{16}$$

where p/τ_0 and q/τ_0 are the corresponding relay and the aerosol weight. With an increase in λ, the aerosol portion of the component noticeably

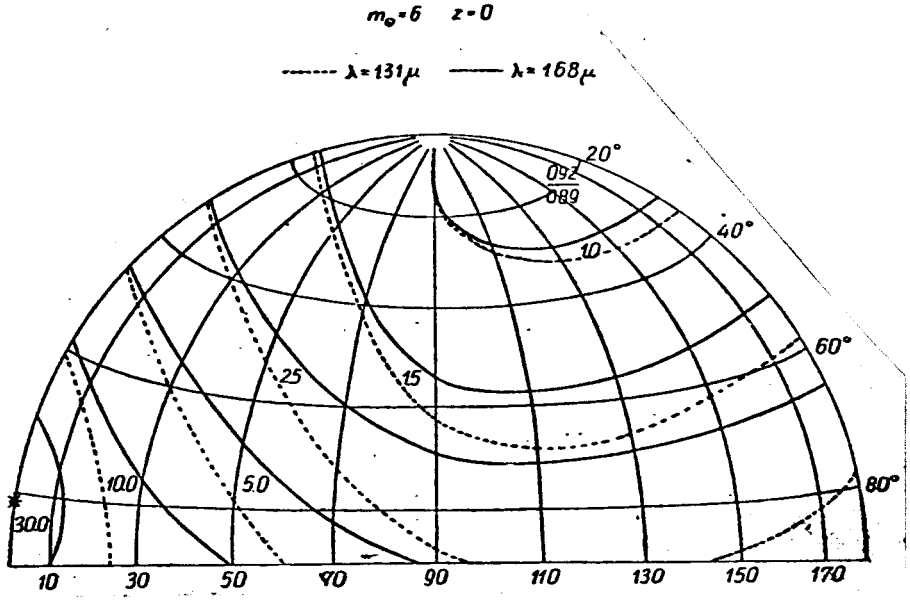

Figure 10. Isophotos of the scattered radiation in the absorption spectrum ψ and outside the spectrum when m = 6, z = 0

increases and correspondingly, the elongation of the indicatrix also increases. Thus, from the data of supplement I in Ref. 4, when the horizontal visibility range is V = 20 km, $\tau_0(\lambda_0) = 0.3$, we obtain the relay and aerosol weights which are given in Table 2. Correspondingly, the values for the atmospheric indicatrix given in Table 3 are obtained from the data in Table 12 of Reference 4, and on the basis of (16).

Table 2. Relay in Aerosol Spectral Weights
When V = 20 km $\tau_0(\lambda_0) = 0.3$

$\lambda(\mu)$	$\frac{p}{\tau_0}$	$\frac{q}{\tau_0}$
0.400	0.554	0.446
0.550	0.317	0.683
0.800	0.129	0.871

Table 3. Changes in the Elongation of the Indicatrix Dependent on the Wavelength

γ \ λ	0.400	0.550	0.800	γ \ λ	0.400	0.550	0.800
0	6.81	9.63	11.9	100	0.579	0.476	0.394
10	5.00	6.87	8.36	110	0.605	0.483	0.384
20	3.40	4.45	5.29	120	0.654	0.504	0.385
30	2.24	2.74	3.13	130	0.722	0.543	0.391
40	1.61	1.83	2.01	140	0.797	0.589	0.424
50	1.20	1.28	1.34	150	0.862	0.637	0.452
60	0.931	0.928	0.926	160	0.930	0.674	0.475
70	0.747	0.699	0.660	170	0.972	0.704	0.491
80	0.640	0.570	0.514	180	0.988	0.716	0.500
90	0.585	0.497	0.428	$\varkappa_1$	0.78	1.18	1.54

The result of these calculations are given in Figure 11, which shows that with the increase of λ, the elongation of the indicatrix also increases. It should be added that, actually, the deformation of the indicatrix with the increase of λ is smaller than that given in Figure 11, since, with the increase of λ, the aerosol indicatrix $\varkappa_a(\gamma)$ will be squeezed in. This effect was not taken into consideration in the above

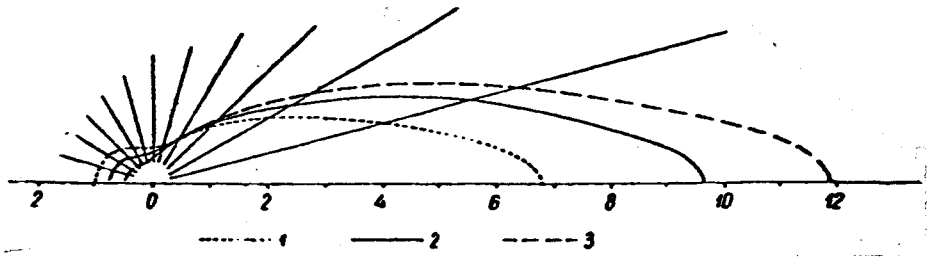

Figure 11. Changes in the elongation of the indicatrix dependent on the wavelength. 1, when $\lambda = 0.400\ \mu$; 2, when $\lambda = 0.550\ \mu$; 3, when $\lambda = 0.800\ \mu$

and since it acts in the opposite direction therefore taken as a whole it will diminish the resulting effect.

It should be pointed out that under certain conditions the change /41
effect can be greater than the effect of the weights, and taken as a whole, the deformation of the indicatrix will be just the opposite from the one discussed above.

In conclusion, it should be noted that the given calculations of the spectral fluxes and the intensities for the standard radiation model of the atmosphere have good coincidence with the mean of the experimental data, and can be successfully used for the various practical problems (for example, for calculating the spectral corrections of the radiation receivers, for evaluating the radiation doses in a spectral interval which interests us, etc.).

Submitted for publication
November 1, 1961

Supplement

/43

Table 1. Subozone Distribution of the Energy in the Direct Solar Radiation Spectrum in Mcal/cm^2·min

$\lambda_1 - \lambda_2$	m							
	„0“	1	1.5	2	2.5	3	4	6
0.29—0.30	9.2	1.0	0.0	0.0	0.0	0.0	0.0	0.0
0.30—0.32	20.6	10.4	7.4	5.3	3.7	2.7	1.3	0.4
0.32—0.34	30.8	28.6	27.6	26.5	25.6	24.7	22.9	19.7
0.34—0.36	33.4	33.3	33.3	33.2	33.1	33.1	33.0	32.8
0.36—0.38	36.4	36.4	36.4	36.4	36.4	36.4	36.4	36.4
0.38—0.40	34.8	34.8	34.8	34.8	34.8	34.8	34.8	34.8
0.29—0.40	165.2	144.5	139.5	136.2	133.6	131.7	128.4	124.1
0.40—0.44	107.5	107.5	107.5	107.5	107.5	107.5	107.5	107.5
0.44—0.48	124.0	123.5	123.3	123.0	122.8	122.5	122.0	121.0
0.48—0.52	114.0	113.0	112.5	111.9	111.5	110.9	110.0	108.0
0.52—0.56	111.0	108.6	107.4	106.2	105.0	103.9	101.7	97.2
0.56—0.60	108.0	104.3	102.5	100.7	98.9	97.2	93.9	87.6
0.60—0.64	98.0	95.2	93.8	92.5	91.1	89.9	87.2	82.3
0.64—0.68	92.0	90.5	89.8	89.1	88.4	87.7	86.3	83.5
0.68—0.70	43.0	42.7	42.6	42.4	42.3	42.1	41.8	41.2
0.40—0.70	797.5	785.3	779.4	773.3	767.5	761.7	750.4	728.3

Table 2. Energy Distribution in the Direct Solar Radiation

/44

Spectrum on the Earth's Surface z = 0 in Mcal/cm^2·min at Various Optical Thicknesses $\tau_0(\lambda_0)$ and Water Vapor Content w

$\lambda_1 - \lambda_2$	m						
	1	1.5	2	2.5	3	4	6
			$\tau_0(\lambda_0) = 0.2$				
0.29—0.30	0.0	0.0	0.0	0.0	0.0	0.0	0.0
0.30—0.32	3.1	1.2	0.5	0.2	0.1	0.0	0.0
0.32—0.34	10.9	6.4	3.9	2.3	1.4	0.4	0.1
0.34—0.36	15.3	10.4	7.0	4.7	3.2	1.5	0.3
0.36—0.38	19.1	13.8	10.0	7.2	5.2	2.8	0.8
0.38—0.40	20.3	15.5	11.9	9.0	6.9	4.0	1.4
0.29—0.40	68.7	47.3	33.3	23.4	16.8	8.7	2.6
0.40—0.44	70.4	57.0	46.1	37.3	30.2	19.8	8.5
0.44—0.48	89.4	75.9	64.5	54.5	46.5	33.6	17.5
0.48—0.52	87.6	76.7	67.2	58.9	51.6	39.8	23.3
0.52—0.56	88.0	78.4	69.9	62.2	55.5	44.1	27.7
0.56—0.60	87.5	78.7	70.7	63.8	57.3	46.5	30.5
0.60—0.64	81.9	74.8	68.3	62.4	57.1	47.7	33.3
0.64—0.68	79.3	73.6	68.5	63.5	59.0	50.9	37.9
0.68—0.70	37.8	35.5	33.3	31.3	29.3	25.8	19.9
0.40—0.70	621.9	550.6	488.5	433.9	386.5	308.2	198.6
			$\tau_0(\lambda_0) = 0.2$,	$w = 0.5$ cm			
0.70—0.74	68.3	64.2	60.2	56.6	53.2	47.1	37.0
0.74—0.79	79.5	75.5	71.8	68.2	64.8	58.5	47.7
0.79—0.84	68.9	64.1	62.2	59.2	56.3	51.0	42.0
0.84—0.86	24.8	23.8	22.8	21.9	21.0	19.3	16.3
0.86—0.99	133.6	125.8	119.1	112.8	107.0	96.7	79.3
0.99—1.03	38.4	37.2	36.0	34.8	33.7	31.6	27.8
1.03—1.23	140.5	133.2	127.0	121.1	116.0	106.4	90.4
1.23—1.25	13.3	13.0	12.7	12.3	12.1	11.5	10.4
1.25—1.38	39.8	35.2	31.9	29.3	27.3	23.6	18.6
1.38—1.50	28.0	24.8	22.4	20.6	19.1	16.6	13.1
1.50—1.53	6.1	5.4	4.9	4.5	4.2	3.7	2.9
1.53—1.54	2.1	1.9	1.8	1.6	1.5	1.3	1.0
1.54—1.67	38.8	37.9	37.2	36.4	35.6	34.1	31.5
1.67—1.70	7.7	7.6	7.5	7.3	7.2	7.0	6.5
1.70—1.92	26.7	24.5	22.9	21.6	20.7	18.8	16.2

Table 2 (Continued)

$\lambda_1 - \lambda_2$	m						
	1	1.5	2	2.5	3	4	6
1.92—2.08	11.6	9.9	8.9	8.0	7.4	6.4	5.0
2.08—2.10	2.3	2.2	2.1	2.0	1.8	1.7	1.4
2.10—2.27	19.5	19.2	18.9	18.7	18.4	18.0	17.0
2.27—2.63	10.2	8.9	8.0	7.3	6.7	5.8	4.4
2.63—2.87	1.5	1.1	0.9	0.8	0.6	0.5	0.3
2.87—3.00	1.8	1.6	1.4	1.2	1.1	1.0	0.9
3.00—3.57	10.1	8.8	7.6	6.7	5.8	4.3	1.8
3.57—4.00	6.9	6.8	6.8	6.7	6.7	6.6	6.4
0.70—4.00	780.4	732.6	695.0	659.6	628.2	571.5	477.9
0.29—4.00	1471	1330	1217	1117	1032	888	679
$f_3(m)\frac{S_m}{S_{id}}$	8	9	9	10	9	9	8
$S_m\Big\vert_{0.29}^{4.00}$	1463	1321	1208	1107	1023	879	671
	$\tau_0(\lambda_0) = 0.2, \quad w = 2.1$ cm						
0.70—0.74	66.2	61.6	57.4	53.6	50.1	43.9	34.0
0.74—0.79	79.5	75.5	71.8	68.2	64.8	58.5	47.7
0.79—0.84	66.4	62.5	58.9	55.7	52.6	47.1	38.2
0.84—0.86	24.8	23.8	22.8	21.9	21.0	19.3	16.3
0.86—0.99	119.5	109.7	101.1	94.2	86.8	75.7	57.9
0.99—1.03	38.4	37.2	36.0	34.8	33.7	31.6	27.8
1.03—1.23	125.2	115.1	107.3	99.9	93.5	82.3	65.1
1.23—1.25	13.3	13.0	12.7	12.3	12.1	11.5	10.4
1.25—1.38	26.8	22.7	19.7	17.3	15.3	12.4	8.6
1.38—1.50	18.9	16.0	13.8	12.2	10.9	8.7	6.1
1.50—1.53	4.0	3.5	3.0	2.6	2.4	2.0	1.3
1.53—1.54	1.4	1.2	1.1	0.9	0.9	0.7	0.5
1.54—1.67	38.8	37.9	37.2	36.4	35.6	34.1	31.5
1.67—1.70	7.7	7.6	7.5	7.3	7.2	7.0	6.5
1.70—1.92	20.6	18.5	17.1	15.8	14.9	13.4	10.7
1.92—2.08	8.9	7.5	6.6	5.8	5.3	4.5	3.5
2.08—2.10	2.3	2.2	2.1	2.0	1.8	1.7	1.4
2.10—2.27	19.5	19.2	18.9	18.7	18.4	18.0	17.0
2.27—2.63	6.1	4.8	4.0	3.3	2.8	1.9	0.9
2.63—2.87	0.9	0.6	0.5	0.4	0.3	0.2	0.1

Table 2 (Continued)

$\lambda_1 - \lambda_2$	m						
	1	1.5	2	2.5	3	4	6
2.87—3.00	1.1	0.9	0.7	0.6	0.5	0.4	0.2
3.00—3.57	4.2	1.6	0.0	0.0	0.0	0.0	0.0
3.57—4.00	6.9	6.8	6.8	6.7	6.7	6.6	6.4
0.70—4.00	701.4	649.4	607.0	570.6	537.6	481.5	392.1
0.29—4.00	1392	1247	1129	1028	941	798	593
$f_3(m)\frac{S_m}{S_{id}}$	8	8	8	8	8	8	7
$S_m\Big\vert_{0.29}^{4.00}$	1384	1239	1121	1020	933	790	586
	$\tau_0(\lambda_0) = 0.2$, $w = 3.0$ cm						
0.70—0.74	65.3	60.6	56.4	52.8	48.9	42.7	32.7
0.74—0.79	79.5	75.5	71.8	68.2	64.8	58.5	47.7
0.79—0.84	65.4	61.3	57.8	54.4	51.2	45.6	36.5
0.84—0.86	24.8	23.8	22.8	21.9	21.0	19.3	16.3
0.86—0.99	114.3	103.6	94.5	86.8	79.9	68.4	50.6
0.99—1.03	38.4	37.2	36.0	34.8	33.7	31.6	27.8
1.03—1.23	119.6	108.9	100.0	92.5	85.6	74.2	56.8
1.23—1.25	13.3	13.0	12.7	12.3	12.1	11.5	10.4
1.25—1.38	23.6	19.6	16.6	14.3	12.4	9.7	6.0
1.38—1.50	16.6	13.7	11.7	10.0	8.7	6.8	4.2
1.50—1.53	3.6	3.0	2.6	2.2	2.0	1.5	0.9
1.53—1.54	1.3	1.0	0.9	0.8	0.7	0.5	0.3
1.54—1.67	38.8	37.9	37.2	36.4	35.6	34.1	31.5
1.67—1.70	7.7	7.6	7.5	7.3	7.2	7.0	6.5
1.70—1.92	19.1	17.1	15.7	14.6	13.6	12.1	9.8
1.92—2.08	8.2	7.0	6.0	5.4	4.8	4.1	3.1
2.08—2.10	2.3	2.2	2.1	2.0	1.8	1.7	1.4
2.10—2.27	19.5	19.2	18.9	18.7	18.4	18.0	17.0
2.27—2.63	5.0	3.9	3.0	2.4	1.8	1.0	0.0
2.63—2.87	1.0	0.5	0.3	0.2	0.2	0.1	0.0
2.87—3.00	0.9	0.7	0.5	0.4	0.3	0.2	0.0
3.00—3.57	2.0	0.0	0.0	0.0	0.0	0.0	0.0
3.57—4.00	6.9	6.8	6.8	6.7	6.7	6.6	6.4
0.70—4.00	677.1	624.1	581.8	545.1	511.4	455.2	365.9
0.29—4.00	1368	1222	1104	1002	915	772	567
$f_3(m)\frac{S_m}{S_{id}}$	8	8	8	8	8	7	7
$S_m\Big\vert_{0.29}^{4.00}$	1360	1214	1096	994	907	765	560

Table 2 (Continued)

/47

$\lambda_1 - \lambda_2$	m						
	1	1.5	2	2.5	3	4	6
			$\tau_0(\lambda_0) = 0.3$				
0.29—0.30	0.0	0.0	0.0	0.0	0.0	0.0	0.0
0.30—0.32	2.6	0.9	0.3	0.1	0.0	0.0	0.0
0.32—0.34	9.2	5.0	2.8	1.5	0.8	0.2	0.0
0.34—0.36	13.1	8.2	5.1	3.2	2.0	0.8	0.1
0.36—0.38	16.5	11.1	7.4	5.0	3.4	1.5	0.3
0.38—0.40	17.6	12.6	8.9	6.4	4.5	2.3	0.6
0.29—0.40	59,0	37.8	24.5	16.2	10.7	4.8	1.0
0.40—0.44	61.8	46.9	35.5	26.9	20.4	11.7	3.9
0.44—0.48	79.3	63.5	50.7	40.5	32.5	20.8	8.5
0.48—0.52	78.4	65.0	53.9	44.8	37.1	25.5	12.2
0.52—0.56	79.6	67.5	57.1	48.4	41.0	29.4	15.2
0.56—0.60	79.6	68.3	58.7	50.4	43.3	31.9	17.4
0.60—0.64	74.9	65.5	57.3	50.0	43.7	33.4	19.5
0.64—0.68	73.0	64.9	57.8	51.5	45.8	36.4	22.9
0.68—0.70	35.0	31.5	28.4	25.6	23.0	18.8	12.4
0.40—0.70	561.6	473.1	399.4	338.1	286.8	207.9	112.0
			$\tau_0(\lambda_0) = 0.3$, $w = 0.5$ cm				
0.70—0.74	63.3	57.4	51.7	47.7	42.4	34.8	23.4
0.74—0.79	73.9	67.8	62.1	56.9	52.2	43.9	31.0
0.79—0.84	64.5	57.9	54.4	50.0	46.0	39.0	28.0
0.84—0.86	23.3	21.6	20.1	18.7	17.3	14.9	11.1
0.86—0.99	125.9	115.1	105.9	97.3	89.6	76.3	55.7
0.99—1.03	36.2	34.0	31.9	30.0	28.2	24.9	19.4
1.03—1.23	133.8	124.0	115.4	107.5	100.5	87.9	67.8
1.23—1.25	12.7	12.2	11.6	11.0	10.5	9.6	7.9
1.25—1.38	38.2	33.1	29.4	26.4	24.1	20.0	14.5
1.38—1.50	27.0	23.4	20.8	18.8	17.1	14.3	10.4
1.50—1.53	5.8	5.1	4.6	4.1	3.7	3.2	2.3
1.53—1.54	2.0	1.8	1.6	1.5	1.4	1.1	0.8
1.54—1.67	37.5	36.0	34.7	33.4	32.2	29.8	25.7
1.67—1.70	7.5	7.2	7.0	6.8	6.5	6.1	5.3
1.70—1.92	25.9	23.5	21.6	20.1	18.9	16.7	13.5
1.92—2.08	11.3	9.5	8.4	7.4	6.8	5.7	4.2
2.08—2.10	2.3	2.1	2.0	1.8	1.7	1.5	1.2
2.10—2.27	19.0	18.5	18.1	17.6	17.2	16.3	14.7
2.27—2.63	9.9	8.6	7.7	6.9	6.3	5.3	3.9
2.63—2.87	1.4	1.0	0.8	0.7	0.5	0.4	0.2
2.87—3.00	1.8	1.5	1.	1.2	1.1	0.9	0.7
3.00—3.57	10.0	8.6	7.4	6.4	5.5	4.0	1.6
3.57—4.00	6.8	6.7	6.6	6.5	6.4	6.2	5.8

Table 2 (Continued)

$\lambda_1 - \lambda_2$	m						
	1	1.5	2	2.5	3	4	6
0.70—4.00	740.0	676.6	625.1	578.7	536.1	462.8	349.1
0.29—4.00	1361	1188	1049	933	834	676	462
$f_3(m)\frac{S_m}{S_{id}}$	8	8	8	8	8	7	6
$S_m\Big\vert_{0.29}^{4.00}$	1353	1180	1041	925	826	669	456
	$\tau_0(\lambda_0) = 0.3, \quad w = 2.1$ cm						
0.70—4.00	740.0	676.6	49.3	45.2	40.0	32.4	21.6
0.74—0.79	73.9	67.8	62.1	56.9	52.2	43.9	31.0
0.79—0.84	62.1	56.5	51.5	47.1	43.0	36.0	25.5
0.84—0.86	23.3	21.6	20.1	18.7	17.3	14.9	11.1
0.86—0.99	112.6	100.4	89.9	81.2	72.8	59.8	40.7
0.99—1.03	36.2	34.0	31.9	30.0	28.2	24.9	19.4
1.03—1.23	119.2	107.2	97.4	88.7	81.0	68.0	48.8
1.23—1.25	12.7	12.2	11.6	11.0	10.5	9.6	7.9
1.25—1.38	25.7	21.4	18.1	15.6	13.7	10.5	6.7
1.38—1.50	18.2	15.1	12.8	11.1	9.8	7.5	4.8
1.50—1.53	3.9	3.3	2.8	2.4	2.1	1.7	1.1
1.53—1.54	1.4	1.2	1.0	0.8	0.8	0.6	0.4
1.54—1.67	37.5	36.0	34.7	33.4	32.2	29.8	25.7
1.67—1.70	7.5	7.2	7.0	6.8	6.5	6.1	5.3
1.70—1.92	20.0	17.7	16.1	14.7	13.6	11.9	8.9
1.92—2.08	8.7	7.2	6.2	5.4	4.9	4.0	3.0
2.08—2.10	2.3	2.1	2.0	1.8	1.7	1.5	1.2
2.10—2.27	19.0	18.5	18.1	17.6	17.2	16.3	14.7
2.27—2.63	5.9	4.7	3.8	3.1	2.6	1.7	0.8
2.63—2.87	0.9	0.6	0.5	0.4	0.3	0.2	0.1
2.87—3.00	1.1	0.9	0.6	0.5	0.4	0.3	0.2
3.00—3.57	4.2	1.5	0.0	0.0	0.0	0.0	0.0
3.57—4.00	6.8	6.7	6.6	6.5	6.4	6.2	5.8
0.70—4.00	664.5	598.8	544.1	498.9	457.2	387.8	284.7
0.29—4.00	1285	1110	968	853	755	600	398
$f_3(m)\frac{S_m}{S_{id}}$	7	7	8	7	6	6	5
$S_m\Big\vert_{0.29}^{4.00}$	1278	1103	960	846	749	594	393

Table 2 (Continued)

$\lambda_1 - \lambda_2$	m						
	1	1.5	2	2.5	3	4	6
	$\tau_0(\lambda_0) = 0.3$, $w = 3.0$ cm						
0.70—0.74	60.5	54.1	48.5	44.5	39.0	31.5	20.7
0.74—0.79	73.9	67.8	62.1	56.9	52.2	43.9	31.0
0.79—0.84	61.2	55.4	50.5	46.0	41.8	34.9	24.4
0.84—0.86	23.3	21.6	20.1	18.7	17.3	14.9	11.1
0.86—0.99	107.7	94.8	84.0	74.8	67.0	54.0	35.5
0.99—1.03	36.2	34.0	31.9	30.0	28.2	24.9	19.4
1.03—1.23	113.9	101.4	90.9	82.0	74.2	61.3	42.6
1.23—1.25	12.7	12.2	11.6	11.0	10.5	9.6	7.9
1.25—1.38	22.6	18.4	15.2	12.9	10.9	8.2	4.6
1.38—1.50	16.0	13.0	10.8	9.1	7.8	5.9	3.3
1.50—1.53	3.4	2.9	2.4	2.0	1.8	1.3	0.8
1.53—1.54	1.2	1.0	0.9	0.7	0.6	0.4	0.3
1.54—1.67	37.5	36.0	34.7	33.4	32.2	29.8	25.7
1.67—1.70	7.5	7.2	7.0	6.8	6.5	6.1	5.3
1.70—1.92	18.5	16.4	14.8	13.5	12.4	10.7	8.2
1.92—2.08	8.0	6.7	5.7	5.0	4.5	3.6	2.6
2.08—2.10	2.3	2.1	2.0	1.8	1.7	1.5	1.2
2.10—2.27	19.0	18.5	18.1	17.6	17.2	16.3	14.7
2.27—2.63	4.9	3.7	2.8	2.2	1.7	0.9	0.0
2.63—2.87	1.0	0.5	0.3	0.2	0.2	0.1	0.0
2.87—3.00	0.9	0.7	0.5	0.4	0.3	0.2	0.0
3.00—3.57	1.9	0.0	0.0	0.0	0.0	0.0	0.0
3.57—4.00	6.8	6.7	6.6	6.5	6.4	6.2	5.8
0.70—4.00	640.9	575.1	521.4	476.0	434.4	366.2	265.1
0.29—4.00	1262	1086	945	830	732	579	378
$f_3(m)\frac{S_m}{S_{id}}$	7	7	7	6	6	6	5
$S_m\Big\vert_{0.29}^{4.00}$	1255	1079	938	824	726	573	373
	$\tau_0(\lambda_0) = 0.5$						
0.29—0.30	0.0	0.0	0.0	0.0	0.0	0.0	0.0
0.30—0.32	1.8	0.5	0.2	0.1	0.0	0.0	0.0
0.32—0.34	6.6	3.0	1.4	0.7	0.3	0.1	0.0
0.34—0.36	9.6	5.1	2.7	1.5	0.8	0.2	0.0
0.36—0.38	12.2	7.1	4.1	2.4	1.4	0.5	0.1
0.38—0.40	13.3	8.2	5.1	3.1	1.9	0.7	0.1
0.29—0.40	43.5	23.9	13.5	7.8	4.4	1.5	0.2

Table 2 (Continued)

/50

$\lambda_1 - \lambda_2$	m						
	1	1.5	2	2.5	3	4	6
0.40—0.44	47.5	31.6	21.1	14.0	9.2	4.1	0.8
0.44—0.48	62.4	44.3	31.4	22.4	15.8	8.0	2.0
0.48—0.52	63.1	47.1	35.0	26.0	19.3	10.8	3.3
0.52—0.56	64.9	49.8	38.0	29.0	22.3	13.0	4.5
0.56—0.60	65.8	51.4	40.1	31.3	24.5	14.9	5.5
0.60—0.64	62.7	50.1	40.1	32.2	25.7	16.5	6.7
0.64—0.68	61.7	50.7	41.6	34.0	27.9	18.8	8.4
0.68—0.70	29.8	24.8	20.6	17.2	14.3	9.8	4.7
0.40—0.70	457.9	349.8	267.9	206.1	159.0	95.9	35.9
	$\tau_0(\lambda_0) = 0.5, \quad w = 0.5$ cm						
0.70—0.74	54.3	45.5	38.0	31.8	26.7	18.8	9.3
0.74—0.79	64.0	54.6	46.5	39.6	33.8	24.6	13.0
0.79—0.84	56.3	47.4	41.6	35.8	30.8	22.9	12.6
0.84—0.86	20.4	17.8	15.5	13.5	11.7	8.9	5.1
0.86—0.99	111.9	96.5	83.7	72.4	62.9	47.6	27.4
0.99—1.03	32.3	28.7	25.4	22.6	20.0	15.7	9.8
1.03—1.23	121.6	107.4	95.2	84.6	75.4	59.8	38.0
1.23—1.25	11.6	10.6	9.7	8.8	8.1	6.7	4.7
1.25—1.38	35.1	29.1	24.9	21.4	18.7	14.3	8.7
1.38—1.50	25.0	20.9	17.8	15.5	13.5	10.5	6.6
1.50—1.53	5.4	4.6	3.9	3.4	3.0	2.4	1.5
1.53—1.54	1.9	1.6	1.4	1.2	1.1	0.8	0.5
1.54—1.67	35.0	32.5	30.2	28.1	26.1	22.6	17.0
1.67—1.70	7.0	6.6	6.1	5.7	5.4	4.7	3.6
1.70—1.92	24.4	21.4	19.1	17.2	15.7	13.1	9.4
1.92—2.08	10.7	8.8	7.5	6.5	5.8	4.6	3.0
2.08—2.10	2.2	2.0	1.8	1.6	1.5	1.2	0.9
2.10—2.27	18.1	17.2	16.3	15.5	14.7	13.3	10.8
2.27—2.63	9.5	8.0	7.0	6.1	5.5	4.6	3.0
2.63—2.87	1.4	1.0	0.8	0.6	0.5	0.4	0.2
2.87—3.00	1.7	1.4	1.2	1.1	1.0	0.8	0.6
3.00—3.57	9.6	8.1	6.9	5.9	5.0	3.5	1.3
3.57—4.00	6.6	6.4	6.2	6.0	5.9	5.5	4.9
0.70—4.00	666.0	578.1	506.7	444.9	392.8	307.3	191.9
0.29—4.00	1167	952	788	659	556	405	228
$f_3(m)\frac{S_m}{S_{id}}$	7	6	6	5	5	4	3
$S_m\Big\|_{0.29}^{4.00}$	1160	946	782	654	551	401	225

Table 2 (Continued)

/51

$\lambda_1 - \lambda_2$	m						
	1	1.5	2	2.5	3	4	6
			$\tau_0(\lambda_0) = 0.5$, $w = 2.1$ cm				
0.70—0.74	52.6	43.6	36.3	30.2	25.7	17.5	8.6
0.74—0.79	64.0	54.6	46.5	39.6	33.8	24.6	13.0
0.79—0.84	54.3	46.2	39.4	33.6	28.8	21.1	11.5
0.84—0.86	20.4	17.8	15.5	13.5	11.7	8.9	5.1
0.86—0.99	100.1	84.1	71.0	60.4	51.0	37.3	20.0
0.99—1.03	32.3	28.7	25.4	22.6	20.0	15.7	9.8
1.03—1.23	108.4	92.8	80.4	70.2	60.7	46.2	27.4
1.23—1.25	11.6	10.6	9.7	8.8	8.1	6.7	4.7
1.25—1.38	23.6	18.8	15.3	12.7	10.7	7.5	4.0
1.38—1.50	16.8	13.4	11.0	9.1	7.7	5.5	3.0
1.50—1.53	3.6	3.0	2.4	2.0	1.7	1.3	0.7
1.53—1.54	1.3	1.0	0.9	0.7	0.6	0.4	0.2
1.54—1.67	35.0	32.5	30.2	28.1	26.1	22.6	17.0
1.67—1.70	7.0	6.6	6.1	5.7	5.4	4.7	3.6
1.70—1.92	18.8	16.2	14.3	12.6	11.3	9.3	6.2
1.92—2.08	8.2	6.6	5.6	4.7	4.1	3.2	2.1
2.08—2.10	2.2	2.0	1.8	1.6	1.5	1.2	0.9
2.10—2.27	18.1	17.2	16.3	15.5	14.7	13.3	10.8
2.27—2.63	5.7	4.4	3.5	2.8	2.3	1.5	0.6
2.63—2.87	0.8	0.5	0.4	0.3	0.2	0.1	0.1
2.87—3.00	1.0	0.8	0.6	0.5	0.4	0.3	0.1
3.00—3.57	4.0	1.4	0.0	0.0	0.0	0.0	0.0
3.57—4.00	6.6	6.4	6.2	6.0	5.9	5.5	4.9
0.70—4.00	596.4	509.2	438.8	381.2	332.4	254.4	154.3
0.29—4.00	1098	883	720	595	496	352	190
$f_3(m)\frac{S_m}{S_{id}}$	6	6	5	5	4	3	2
$S_m\Big\vert_{0.29}^{4.00}$	1092	877	715	590	492	349	188
			$\tau_0(\lambda_0) = 0.5$, $w = 3.0$ cm				
0.70—0.74	51.9	42.9	35.7	29.7	24.5	17.1	8.2
0.74—0.79	64.0	54.6	46.5	39.6	33.8	24.6	13.0
0.79—0.84	53.5	45.3	38.6	32.9	28.0	20.4	10.9
0.84—0.86	20.4	17.8	15.5	13.5	11.7	8.9	5.1
0.86—0.99	95.7	79.4	66.4	55.7	47.0	33.7	17.5
0.99—1.03	32.3	28.7	25.4	22.6	20.0	15.7	9.8
1.03—1.23	103.5	87.8	75.0	64.6	55.6	41.7	23.9
1.23—1.25	11.6	10.6	9.7	8.8	8.1	6.7	4.7
1.25—1.38	20.8	16.2	12.9	10.4	8.5	5.9	2.8
1.38—1.50	14.8	11.5	9.3	7.5	6.2	4.3	2.1

Table 2 (Continued)

$\lambda_1 - \lambda_2$	m						
	1	1.5	2	2.5	3	4	6
1.50—1.53	3.2	2.6	2.1	1.7	1.4	1.0	0.5
1.53—1.54	1.1	0.9	0.7	0.6	0.5	0.3	0.2
1.54—1.67	35.0	32.5	30.2	28.1	26.1	22.6	17.0
1.67—1.70	7.0	6.6	6.1	5.7	5.4	4.7	3.6
1.70—1.92	17.4	14.9	13.1	11.6	10.3	8.4	5.7
1.92—2.08	7.6	6.2	5.1	4.4	3.8	2.9	1.9
2.08—2.10	2.2	2.0	1.8	1.6	1.5	1.2	0.9
2.10—2.27	18.1	17.2	16.3	15.5	14.7	13.3	10.8
2.27—2.63	4.7	3.5	2.6	2.0	1.4	0.8	0.0
2.63—2.87	0.9	0.4	0.3	0.2	0.2	0.1	0.0
2.87—3.00	0.8	0.6	0.4	0.3	0.2	0.1	0.0
3.00—3.57	1.9	0.0	0.0	0.0	0.0	0.0	0.0
3.57—4.00	6.6	6.4	6.2	6.0	5.9	5.5	4.9
0.70—4.00	575.0	488.6	419.9	363.0	314.8	239.9	143.5
0.29—4.00	1076	862	701	577	478	337	180
$f_3(m)\frac{S_m}{S_{id}}$	6	6	5	5	4	3	2
$S_m\Big\vert_{0.29}^{4.00}$	1070	856	696	572	474	334	178

Table 3. Energy Distribution in the Direct Solar Radiation Spectrum at Various Levels in Mcal/cm^2·min for the Standard Radiation Model of the Atmosphere ($\tau_0(\lambda_0) = 0.3$, w = 2.1 cm)

$\lambda_1 - \lambda_2$	m						
	1	1.5	2	2.5	3	4	6
			$z = 0.5$ km				
0.29—0.30	0.0	0.0	0.0	0.0	0.0	0.0	0.0
0.30—0.32	3.2	1.2	0.5	0.0	0.0	0.0	0.0
0.32—0.34	11.0	6.5	3.9	2.3	1.4	0.5	0.0
0.34—0.36	15.2	10.3	6.9	4.7	3.2	1.4	0.2
0.36—0.38	18.9	13.6	9.8	7.0	5.1	2.6	0.7
0.38—0.40	20.0	15.2	11.5	8.8	6.6	3.8	1.3
0.29—0.40	68.3	46.8	32.6	22.8	16.3	8.3	2.2

Table 3 (Continued)

/53

$\lambda_1 - \lambda_2$	m						
	1	1.5	2	2.5	3	4	6
0.40—0.44	69.1	55.4	44.4	35.6	28.5	18.4	7.6
0.44—0.48	87.5	73.6	61.8	52.0	43.7	30.8	15.3
0.48—0.42	85.5	74.1	64.2	55.6	48.2	36.2	20.4
0.52—0.56	86.1	75.9	66.8	58.7	51.8	40.2	24.2
0.56—0.60	85.7	76.2	67.8	60.5	53.8	42.7	26.8
0.60—0.64	80.0	72.3	68.9	59.1	53.5	43.6	29.1
0.64—0.68	78.0	71.4	65.8	60.4	55.6	47.0	33.6
0.68—0.70	37.0	34.5	31.9	29.7	27.6	23.8	17.7
0.40—0.70	608.9	533.4	471.6	411.6	362.7	282.7	174.7
0.70—0.74	65.3	60.3	55.7	51.5	47.7	41.0	30.4
0.74—0.79	78.0	73.5	69.2	65.2	61.4	54.5	42.8
0.79—0.84	65.9	61.7	57.8	54.2	50.9	45.0	35.3
0.84—0.86	24.4	23.2	22.1	21.0	19.9	18.0	14.7
0.86—0.99	121.3	111.2	102.2	94.8	88.0	76.2	57.9
0.99—1.03	37.8	36.3	34.9	33.5	32.2	29.7	25.2
1.03—1.23	127.4	117.6	109.4	102.1	95.5	84.0	66.2
1.23—1.25	13.1	12.7	12.3	12.0	11.6	10.8	9.6
1.25—1.38	29.1	24.6	21.6	19.1	17.1	14.0	9.8
1.38—1.50	20.7	17.5	15.4	13.7	12.3	10.0	7.1
1.50—1.53	4.5	3.8	3.3	2.9	2.7	2.2	1.5
1.53—1.54	1.6	1.4	1.2	1.1	1.0	0.8	0.5
1.54—1.67	38.4	37.5	36.6	35.6	34.7	33.1	30.0
1.67—1.70	7.6	7.5	7.3	7.1	7.0	6.7	6.1
1.70—1.92	21.7	19.5	18.1	16.8	15.8	14.0	11.6
1.92—2.08	9.6	8.1	7.1	6.4	5.7	4.8	3.7
2.08—2.10	2.4	2.2	2.1	1.9	1.8	1.7	1.5
2.10—2.27	19.4	19.0	18.7	18.4	18.1	17.5	16.4
2.27—2.63	6.9	5.6	4.7	4.1	3.5	2.7	1.5
2.63—2.87	1.0	0.7	0.6	0.4	0.4	0.2	0.1
2.87—3.00	1.2	1.0	0.9	0.8	0.6	0.5	0.3
3.00—3.57	5.8	3.5	1.6	0.0	0.0	0.0	0.0
3.57—4.00	6.9	6.8	6.7	6.7	6.6	6.5	6.2
0.70—4.00	710.0	655.2	609.5	569.3	534.5	473.9	378.4
0.29—4.00	1387	1235	1114	1004	914	765	555
			$z = 3$ km				
0.29—0.30	0.1	0.0	0.0	0.0	0.0	0.0	0.0
0.30—0.32	4.8	2.4	1.1	0.6	0.3	0.1	0.0
0.32—0.34	15.2	10.6	7.5	5.3	3.7	1.8	0.5
0.34—0.36	19.9	15.4	11.9	9.2	7.1	4.2	1.5
0.36—0.38	23.9	19.3	15.7	12.7	10.3	6.8	2.9
0.38—0.40	24.6	20.6	17.4	14.8	12.2	8.7	4.3
0.29—0.40	88.5	68.3	53.6	42.6	33.6	21.6	9.2

Table 3 (Continued

/54

$\lambda_1 - \lambda_2$	m						
	1	1.5	2	2.5	3	4	6
0.40—0.44	82.0	71.6	62.6	54.6	47.7	36.3	21.2
0.44—0.48	100.7	90.6	81.6	73.6	66.3	53.7	35.3
0.48—0.52	96.4	88.7	81.7	75.1	69.1	58.4	41.8
0.52—0.56	95.6	88.6	82.3	76.4	70.8	60.9	45.2
0.56—0.60	94.0	87.6	81.6	76.1	70.9	61.7	46.6
0.60—0.64	87.2	82.4	77.5	73.1	69.0	61.4	48.5
0.64—0.68	83.8	80.0	76.4	72.9	69.6	63.4	52.6
0.68—0.70	39.7	38.3	36.8	35.4	34.0	31.5	26.9
0.40—0.70	679.4	627.8	580.5	537.2	497.4	427.3	318.1
0.70—0.74	71.3	68.8	65.9	63.7	61.3	56.8	48.8
0.74—0.79	83.0	80.6	78.2	75.9	73.7	69.5	61.8
0.79—0.84	72.0	69.6	67.1	65.4	63.4	59.7	53 2
0.84—0.86	25.7	25.1	24.5	23.9	23.4	22.3	20.2
0.86—0.99	139.5	133.8	126.1	124.2	120.2	112.0	98.7
0.99—1.03	39.5	38.8	38.1	37.4	36.7	35.3	32.8
1.03—1.23	145.6	140.6	133.7	131.5	127.6	120.6	108.5
1.23—1.25	13.6	13.4	13.2	13.0	12.8	12.5	11.8
1.25—1.38	42.9	38.6	35.4	33.0	31.0	27.8	23.2
1.38—1.50	30.3	27.2	23.5	23.2	21.7	19.6	16.3
1.50—1.53	6.4	5.8	5.1	5.0	4.7	4.2	3.6
1.53—1.54	2.3	2.1	1.8	1.8	1.7	1.5	1.2
1.54—1.67	39.6	39.1	38.6	38.1	37.7	36.8	35.1
1.67—1.70	7.8	7.8	7.7	7.6	7.5	7.4	7.1
1.70—1.92	29.3	26.1	23.8	23.6	22.6	21.1	18.9
1.92—2.08	13.7	11.8	10.8	9.8	9.1	8.1	6.6
2.08—2.10	2.6	2.4	2.3	2.2	2.2	2.1	1.8
2.10—2.27	19.7	19.6	19.4	19.3	19.2	18.9	18.4
2.27—2.63	11.0	10.2	8.3	7.7	7.0	6.2	4.9
2.63—2.87	1.9	1.6	1.3	1.1	0.9	0.8	0.5
2.87—3.00	1.9	1.8	1.6	1.5	1.4	1.2	0.9
3.00—3.57	10.8	9.7	8.6	7.8	7.0	5.7	3.4
3.57—4.00	6.9	6.9	6.9	6.9	6.8	6.8	6.7
0.70—4.00	817.3	781.4	741.9	723.6	699.6	656.9	584.4
0.29—4.00	1585	1478	1376	1303	1231	1106	912
			$z = 6.5$ km				
0.29—0.30	0.1	0.0	0.0	0.0	0.0	0.0	0.0
0.30—0.32	6.7	3.9	2.2	1.2	0.7	0.2	0.0
0.32—0.34	19.2	15.2	12.0	9.5	7.5	4.7	1.8
0.34—0.36	24.0	20.4	17.4	14.8	12.5	9.1	4.7
0.36—0.38	27.9	24.5	21.4	18.8	16.5	12.6	7.4
0.38—0.40	27.9	25.1	22.4	20.1	18.0	14.5	9.4
0.29—0.40	105.8	89.1	75.4	64.4	55.2	41.1	23.3

Table 3 (Continued)

/55

$\lambda_1 - \lambda_2$	m						
	1	1.5	2	2.5	3	4	6
0.40—0.44	90.8	83.5	76.9	70.6	64.9	54.9	39.2
0.44—0.48	109.0	102.1	95.5	89.6	83.9	73.7	56.9
0.48—0.52	102.7	97.3	92.4	87.7	83.3	74.8	60.7
0.52—0.56	100.7	95.8	91.3	87.2	83.0	75.3	62.0
0.56—0.60	98.2	93.6	89.3	85.1	81.2	73.8	61.0
0.60—0.64	90.4	87.0	83.5	80.3	77.1	71.2	60.7
0.64—0.68	86.7	84.0	81.6	79.2	76.8	72.4	64.1
0.68—0.70	40.9	40.0	39.0	38.1	37.2	35.4	32.2
0.40—0.70	719.4	683.3	649.5	617.8	587.4	531.5	436.8
0.70—0.74	75.2	73.5	71.9	70.3	68.8	65.9	60.6
0.74—0.79	85.0	83.5	82.0	80.6	79.2	76.5	71.4
0.79—0.84	74.9	73.6	72.5	71.2	70.1	67.8	63.7
0.84—0.86	26.3	25.9	25.6	25.2	24.9	24.2	23.0
0.86—0.99	150.2	147.3	144.6	142.1	139.6	135.0	126.7
0.99—1.03	40.1	39.7	39.3	38.9	38.5	37.7	36.2
1.03—1.23	156.7	154.0	151.8	149.9	147.6	143.6	136.4
1.23—1.25	13.8	13.7	13.6	13.5	13.3	13.1	12.7
1.25—1.38	59.6	56.0	53.8	51.5	49.0	46.4	41.4
1.38—1.50	42.0	39.6	37.9	36.3	34.5	32.9	29.1
1.50—1.53	9.0	8.4	8.1	7.7	7.4	7.1	6.3
1.53—1.54	3.2	3.0	2.9	2.8	2.7	2.5	2.2
1.54—1.67	40.2	39.9	39.5	39.3	39.0	38.4	37.4
1.67—1.70	7.9	7.9	7.8	7.8	7.8	7.7	7.5
1.70—1.92	36.5	34.7	33.3	32.2	31.2	29.8	27.4
1.92—2.08	17.8	16.6	15.9	15.0	14.4	13.2	11.4
2.08—2.10	2.8	2.7	2.7	2.5	2.5	2.4	2.2
2.10—2.27	19.8	19.8	19.7	19.6	19.5	19.4	19.1
2.27—2.63	16.8	15.4	14.6	13.9	13.3	12.3	11.0
2.63—2.87	3.5	3.0	2.6	2.4	2.2	1.9	1.4
2.87—3.00	2.9	2.7	2.6	2.5	2.4	2.1	1.9
3.00—3.57	14.0	13.5	13.2	12.8	12.5	11.9	11.0
3.57—4.00	7.0	6.9	6.9	6.9	6.9	6.9	6.8
0.70—4.00	905.2	881.3	862.8	844.9	827.3	798.7	746.8
0.29—4.00	1730	1654	1588	1527	1470	1371	1207
			$z = 9$ km				
0.29—0.30	0.2	0.0	0.0	0.0	0.0	0.0	0.0
0.30—0.32	8.0	5.0	3.1	1.9	1.2	0.5	0.0
0.32—0.34	21.8	18.3	15.4	12.9	10.9	7.7	3.9
0.34—0.36	26.7	23.8	21.2	19.0	17.0	13.5	8.6
0.36—0.38	30.4	27.7	25.3	23.2	21.1	17.7	12.3
0.38—0.40	30.0	27.9	25.9	24.1	22.4	19.3	14.4
0.29—0.40	117.1	102.7	90.9	81.1	72.6	58.7	39.2

Table 3 (Continued)

$\lambda_1 - \lambda_2$	m						
	1	1.5	2	2.5	3	4	6
0.40—0.44	96.1	91.1	86.1	81.4	77.1	68.9	55.3
0.44—0.48	113.9	109.2	104.7	100.3	96.1	88.2	74.4
0.48—0.52	106.3	102.7	99.1	95.6	92.3	86.1	74.8
0.52—0.56	103.9	100.6	97.3	94.1	91.0	85.3	74.7
0.56—0.60	100.9	97.6	94.0	91.1	88.0	82.3	71.8
0.60—0.64	92.6	89.9	87.4	85.0	82.6	78.0	69.6
0.64—0.68	88.2	86.5	84.7	83.0	81.3	77.8	71.9
0.68—0.70	41.7	41.2	40.6	40.0	39.4	38.3	36.2
0.40—0.70	743.6	718.8	693.9	670.5	647.8	604.9	528.7
0.70—0.74	76.9	75.9	74.9	74.0	73.1	71.3	68.0
0.74—0.79	86.4	85.6	84.9	84.1	83.3	81.9	79.0
0.79—0.84	76.4	75.8	75.1	74.4	73.9	72.6	70.4
0.84—0.86	26.6	26.4	26.2	26.1	25.9	25.5	24.8
0.86—0.99	154.2	153.0	151.8	150.5	149.3	146.9	142.4
0.99—1.03	40.5	40.3	40.1	39.9	39.7	39.2	38.4
1.03—1.23	160.4	159.2	158.3	157.4	156.1	154.0	150.0
1.23—1.25	13.9	13.9	13.8	13.7	13.7	13.6	13.4
1.25—1.38	66.3	63.8	62.7	61.5	60.4	59.1	55.6
1.38—1.50	47.0	45.2	44.4	43.4	42.6	41.7	39.3
1.50—1.53	10.0	9.6	9.5	9.3	9.2	9.0	8.4
1.53—1.54	3.6	3.5	3.5	3.4	3.3	3.2	3.0
1.54—1.67	40.6	40.5	40.2	40.1	40.0	39.7	39.2
1.67—1.70	8.0	7.9	7.9	7.9	7.9	7.8	7.8
1.70—1.92	41.7	40.8	39.7	38.8	37.9	36.5	34.7
1.92—2.08	20.9	20.1	19.3	18.7	18.1	17.1	15.8
2.08—2.10	2.8	2.8	2.7	2.7	2.7	2.6	2.4
2.10—2.27	19.9	19.9	19.8	19.8	19.8	19.7	19.5
2.27—2.63	21.7	20.0	19.1	18.4	17.8	16.9	15.6
2.63—2.87	5.2	4.4	3.9	3.8	3.4	3.0	2.5
2.87—3.00	3.8	3.5	3.3	3.2	3.1	2.9	2.7
3.00—3.57	15.1	14.8	14.6	14.4	14.3	13.9	13.5
3.57—4.00	7.0	7.0	7.0	7.0	7.0	6.9	6.9
0.70—4.00	948.9	933.9	922.7	912.5	902.5	885.0	853.3
0.29—4.00	1810	1755	1708	1664	1623	1549	1421
			$z = 20$ km				
0.29—0.30	0.4	0.0	0.0	0.0	0.0	0.0	0.0
0.30—0.32	11.7	8.8	6.6	5.0	3.8	2.2	0.7
0.32—0.34	27.3	25.8	24.3	22.8	21.6	19.2	15.1
0.34—0.36	31.6	30.8	29.9	29.2	28.4	26.9	24.1
0.36—0.38	34.9	34.2	33.5	32.9	32.2	30.9	28.5
0.38—0.40	33.7	33.1	32.6	32.1	31.5	30.5	28.5
0.29—0.40	139.6	132.7	126.9	122.0	117.5	109.7	96.9

Table 3 (Continued)

/57

$\lambda_1 - \lambda_2$	m						
	1	1.5	2	2.5	3	4	6
0.40—0.44	104.9	103.7	102.4	101.3	100.1	97.6	93.1
0.44—0.48	121.5	120.3	119.2	117.9	116.7	114.4	110.0
0.48—0.52	111.9	110.9	110.0	108.9	108.0	106.0	102.4
0.52—0.56	108.4	107.0	105.7	104.6	103.2	100.9	96.1
0.56—0.60	104.7	103.0	101.5	99.9	98.5	95.4	89.7
0.60—0.64	95.6	94.3	93.2	92.1	90.9	88.6	84.4
0.64—0.68	90.6	89.8	89.3	88.5	88.0	86.6	84.1
0.68—0.70	42.7	42.5	42.3	42.1	42.0	41.7	40.9
0.40—0.70	780.3	771.5	763.6	755.3	747.4	731.2	700.7
0.70—0.74	78.8	78.7	78.5	78.4	78.3	78.1	77.6
0.74—0.79	87.8	87.7	87.6	87.6	87.5	87.3	86.9
0.79—0.84	77.8	77.8	77.7	77.6	77.5	77.4	77.1
0.84—0.86	27.0	26.9	26.9	26.9	26.9	26.8	26.7
0.86—0.99	158.8	158.7	158.7	158.7	158.5	157.7	157.1
0.99—1.03	41.0	40.9	40.9	40.9	40.9	40.7	40.5
1.03—1.23	164.1	163.9	163.7	163.7	163.3	163.0	162.4
1.23—1.25	14.0	14.0	14.0	14.0	14.0	14.0	14.0
1.25—1.38	71.4	71.2	70.8	70.4	70.2	69.9	69.1
1.38—1.50	50.6	50.4	50.2	49.9	49.7	49.3	48.7
1.50—1.53	10.8	10.7	10.7	10.6	10.6	10.5	10.4
1.53—1.54	3.9	3.9	3.9	3.8	3.8	3.8	3.7
1.54—1.67	40.8	40.8	40.8	40.8	40.7	40.7	40.6
1.67—1.70	8.0	8.0	8.0	8.0	8.0	8.0	8.0
1.70—1.92	45.7	45.4	45.2	44.9	44.7	44.4	43.8
1.92—2.08	23.4	23.0	22.7	22.5	22.2	21.8	21.1
2.08—2.10	2.9	2.9	2.8	2.8	2.8	2.8	2.7
2.10—2.27	20.0	20.0	20.0	20.0	20.0	20.0	20.0
2.27—2.63	27.2	26.9	26.5	26.1	25.9	25.4	24.6
2.63—2.87	7.6	7.0	6.5	6.2	5.9	5.4	4.8
2.87—3.00	4.7	4.6	4.6	4.5	4.5	4.4	4.2
3.00—3.57	15.8	15.7	15.7	15.6	15.6	15.5	15.3
3.57—4.00	7.0	7.0	7.0	7.0	7.0	7.0	7.0
0.70—4.00	989.1	986.1	983.4	980.9	978.5	973.9	966.3
0.29—4.00	1909	1890	1874	1858	1843	1815	1764

Table 4. Values of the Optical Thickness τ_0 of the Spectral Albedo A_λ^{summer} and A_λ^{winter} after Dirmhir (Ref. 18), and Energy Distribution in the Scattered Radiation Spectrum on the Surface of the Earth When m = 2 for the Standard Radiation Model of the Atmosphere ($\tau_0(\lambda_0) = 0.3$, w = 2.1 cm) in Mcal/cm^2·min. Albedo Values are Extrapolated and Given in Parentheses

/58

$\lambda_1 - \lambda_2$	τ_0	A_λ^*	A_λ^{**}	$F_D(A_\lambda^*)$	$F_D(A_\lambda^{**})$
0.29—0.30	1.558	0.02	0.66	0.00	0.00
0.30—0.32	1.389	0.02	0.66	0.89	1.26
0.32—0.34	1.131	0.03	0.67	4.68	6.55
0.34—0.36	0.937	0.03	0.68	6.08	8.26
0.36—0.38	0.794	0.04	0.69	6.64	8.90
0.38—0.40	0.679	0.04	0.70	6.20	8.26
0.29—0.40				24.49	33.23
0.40—0.44	0.554	0.05	0.71	18.16	23.89
0.44—0.48	0.443	0.05	0.72	18.97	24.83
0.48—0.52	0.366	0.06	0.73	15.70	20.39
0.52—0.56	0.310	0.12	0.73	13.86	17.49
0.56—0.60	0.270	0.11	0.72	11.98	15.12
0.60—0.64	0.239	0.09	0.71	10.12	12.77
0.64—0.68	0.215	0.08	0.68	8.94	11.21
0.68—0.70	0.201	0.17	0.65	4.18	5.00
0.40—0.70				101.91	130.70
0.70—0.74	0.191	0.20	0.62	5.53	6.52
0.74—0.79	0.175	0.35	0.55	8.42	9.01
0.79—0.84	0.156	0.46	0.50	5.24	5.32
0.84—0.86	0.149	0.48	0.45	2.35	2.33
0.86—0.99	0.133	0.51	0.36	6.99	6.70
0.99—1.03	0.124	0.52	0.28	3.14	2.87
1.03—1.23	0.104	0.52	0.23	5.95	5.55
1.23—1.25	0.095	0.48	0.16	0.84	0.74
1.25—1.38	0.089	0.44	0.12	0.58	0.68
1.38—1.50	0.080	0.31	0.10	0.36	0.36
1.50—1.53	0.077	0.27	0.08	0.07	0.07
1.53—1.54	0.076	0.28	0.09	0.02	0.02
1.54—1.67	0.071	0.31	0.10	1.58	1.46
1.67—1.70	0.068	0.35	1.12	0.34	0.31
1.70—1.92	0.063	0.30	0.11	0.36	0.36
1.92—2.08	0.058	0.15	0.07	0.13	0.11
2.08—2.10	0.054	0.17	0.08	0.06	0.06
2.10—2.27	0.051	0.20	0.09	0.61	0.60
2.27—2.63	0.046	0.16	0.06	0.04	0.04
2.63—2.87	0.041	0.10	0.04	0.00	0.00
2.87—3.00	0.038	(0.08)	(0.04)	0.06	0.06
3.00—3.57	0.034	(0.07)	(0.03)	0.02	0.02
3.57—4.00	0.030	(0.05)	(0.03)	0.11	0.12
0.70—4.00				42.80	43.31
0.29—4.00				169.2	207.2

* Summer

** Winter

Table 5. Relative Energy Distribution in the Direct Solar Scattered Radiation Spectrum on the Surface of the Earth z = 0 for the Standard Radiation Model of the Atmosphere $\tau_0(\lambda_0) = 0.3$, w = 2.1 cm

/59

$\lambda_1 - \lambda_2$	$\frac{I_\lambda}{(I_\lambda)_{max}}$			$\frac{F^*_{D,\lambda}}{(F^*_{D,\lambda})_{max}}$	$\frac{F^{**}_{D,\lambda}}{(F^{**}_{D,\lambda})_{max}}$
	$m = 1.5$	$m = 2$	$m = 4$	$m = 2$	$m = 2$
0.29—0.30	0.0000	0.0000	0.0000	0.0000	0.0000
0.30—0.32	0.0264	0.0010	0.0000	0.0939	0.1014
0.32—0.34	0.1464	0.0954	0.0106	0.4937	0.5250
0.34—0.36	0.2401	0.1738	0.0426	0.6413	0.6651
0.36—0.38	0.3250	0.2521	0.0798	0.7004	0.7166
0.38—0.40	0.3689	0.3032	0.1223	0.6540	0.6651
0.40—0.44	0.6866	0.6048	0.3110	0.9578	0.9614
0.44—0.48	0.9297	0.8637	0.5340	1.0000	1.0000
0.48—0.52	0.9516	0.9182	0.6781	0.8270	0.8209
0.52—0.56	0.9883	0.9727	0.7819	0.7300	0.7037
0.56—0.60	1.0000	1.0000	0.8484	0.6266	0.6087
0.60—0.64	0.9590	0.9761	0.8883	0.5338	0.5137
0.64—0.68	0.9502	0.9847	0.9681	0.4705	0.4509
0.68—0.70	0.9224	0.9676	1.0000	0.4409	0.4026
0.70—0.74	0.8053	0.9080	0.8617	0.2911	0.2625
0.74—0.79	0.7941	0.8463	0.9340	0.3544	0.2899
0.79—0.84	0.6618	0.7019	0.7660	0.2215	0.1707
0.84—0.86	0.6325	0.6848	0.7926	0.2489	0.1876
0.86—0.99	0.4523	0.4712	0.4894	0.1135	0.0829
0.99—1.03	0.4978	0.5434	0.6649	0.1656	0.1156
1.03—1.23	0.3140	0.3319	0.3617	0.0629	0.0448
1.23—1.25	0.3572	0.3952	0.5106	0.0886	0.0596
1.25—1.38	0.0964	0.0949	0.0860	0.0095	0.0084
1.38—1.50	0.0737	0.0727	0.0665	0.0063	0.0048
1.50—1.53	0.0644	0.0636	0.0603	0.0049	0.0037
1.53—1.54	0.0703	0.0681	0.0638	0.0042	0.0032
1.54—1.67	0.1622	0.1817	0.2438	0.0253	0.0180
1.67—1.70	0.1405	0.1590	0.2163	0.0232	0.0166
1.70—1.92	0.0471	0.0499	0.0576	0.0030	0.0023
1.92—2.08	0.0263	0.0264	0.0266	0.0017	0.0011
2.08—2.10	0.0615	0.0681	0.0798	0.0063	0.0048
2.10—2.27	0.0637	0.0726	0.1020	0.0092	0.0056
2.27—2.63	0.0076	0.0072	0.0050	0.0002	0.0002
2.63—2.87	0.0015	0.0014	0.0008	0.0000	0.0000
2.87—3.00	0.0023	0.0018	0.0014	0.0006	0.0005
3.00—3.57	0.0015	0.0000	0.0000	0.0000	0.0000
3.57—4.00	0.0091	0.0104	0.0153	0.0006	0.0005

* Summer

** Winter

Table 6. Relative Spectral Distribution (Standardized after Integral Flux) of the Direct Solar and Scattered Radiations (summer and winter) on the Surface of the Earth for the Mean Standard Radiation Model of the Atmosphere $\tau_0(\lambda_0) = 0.3$, w = 2.1 cm, When m = 2

/60

$\lambda_1 - \lambda_2$	$\frac{I_\lambda}{S_m}$	$\frac{F^*_{D,\lambda}}{F^*_D}$	$\frac{F^{**}_{D,\lambda}}{F^{**}_D}$
0.29—0.30	0.0000	0.0000	0.0000
0.30—0.32	0.0003	0.0053	0.0061
0.32—0.34	0.0029	0.0277	0.0316
0.34—0.36	0.0053	0.0359	0.0399
0.36—0.38	0.0076	0.0392	0.0429
0.38—0.40	0.0092	0.0366	0.0399
0.40—0.44	0.0367	0.1073	0.1153
0.44—0.48	0.0524	0.1121	0.1198
0.48—0.52	0.0557	0.0928	0.0984
0.52—0.56	0.0590	0.0819	0.0844
0.56—0.60	0.0606	0.0708	0.0730
0.60—0.64	0.0592	0.0598	0.0616
0.64—0.68	0.0597	0.0528	0.0541
0.68—0.70	0.0293	0.0247	0.0241
0.70—0.74	0.0509	0.0327	0.0315
0.74—0.79	0.0642	0.0498	0.0435
0.79—0.84	0.0532	0.0310	0.0257
0.84—0.86	0.0208	0.0139	0.0112
0.86—0.99	0.0929	0.0413	0.0323
0.99—1.03	0.0330	0.0186	0.0138
1.03—1.23	0.1007	0.0352	0.0268
1.23—1.25	0.0120	0.0050	0.0036
1.25—1.38	0.0187	0.0034	0.0033
1.38—1.50	0.0132	0.0021	0.0017
1.50—1.53	0.0029	0.0004	0.0003
1.53—1.54	0.0010	0.0001	0.0001
1.54—1.67	0.0358	0.0093	0.0070
1.67—1.70	0.0072	0.0020	0.0015
1.70—1.92	0.0166	0.0021	0.0017
1.92—2.08	0.0064	0.0008	0.0005
2.08—2.10	0.0021	0.0004	0.0003
2.10—2.27	0.0187	0.0036	0.0029
2.27—2.63	0.0039	0.0002	0.0002
2.63—2.87	0.0005	0.0000	0.0000
2.87—3.00	0.0006	0.0004	0.0003
3.00—3.57	0.0000	0.0001	0.0001
3.57—4.00	0.0068	0.0007	0.0006
0.29—4.00	1.0000	1.0000	1.0000

* Summer

** Winter

Table 7. Relative Distribution of the Intensity of the Descending Scatter Radiation for the Standard Radiation Model of the Atmosphere $\tau_0(\lambda_0) = 0.3$, w = 2.1 cm and Scatter Indicatrix $\overline{\varkappa_{VII}(\gamma)}$, $\varkappa_1 = 0.967$, Albedo A = 0. (Intensities in the Azimuth I_c are Given in Mcal/cm^2·min·μ·sterad)

/61

ϑ \ φ	0	45	90	135	180
		$z=0$, $m=2$			
		$\lambda=0.72$ μ, $I_c=19.1$			
15	1.56	1.34	1.00	0.78	0.71
30	2.87	1.86	1.01	0.67	0.64
45	6.46	2.53	1.06	0.76	0.75
60	14.26	3.27	1.23	0.99	1.01
75	13.34	4.36	1.72	1.57	1.79
		$\lambda=0.76$ μ, $I_c=17.7$			
15	1.57	1.34	1.00	0.78	0.72
30	2.90	1.88	1.02	0.68	0.65
45	6.54	2.56	1.07	0.77	0.76
60	14.68	3.37	1.26	1.02	1.04
75	14.23	4.65	1.84	1.68	1.91
		$\lambda=0.82$ μ, $I_c=12.9$			
15	1.57	1.34	1.00	0.78	0.72
30	2.89	1.87	1.01	0.68	0.65
45	6.50	2.54	1.06	0.76	0.76
60	14.48	3.32	1.24	1.00	1.03
75	13.88	4.53	1.79	1.64	1.86
		$\lambda=0.85$ μ, $I_c=11.9$			
15	1.56	1.34	1.00	0.78	0.72
30	2.91	1.88	1.02	0.68	0.65
45	6.59	2.58	1.08	0.77	0.77
60	14.85	3.41	1.28	1.03	1.05
75	14.81	4.84	1.91	1.75	1.98
		$\lambda=0.93$ μ, $I_c=7.2$			
15	1.56	1.34	1.00	0.78	0.72
30	2.87	1.86	1.01	0.67	0.64
45	6.39	2.50	1.04	0.75	0.74
60	13.71	3.15	1.18	0.95	0.97
75	12.45	4.07	1.61	1.47	1.67

Table 7 (Continued)

/62

ϑ \ φ	0	45	90	135	180
		$\lambda = 1.01\ \mu$, $I_c = 7.7$			
15	1.56	1.34	1.00	0.78	0.72
30	2.90	1.87	1.02	0.68	0.65
45	6.59	2.58	1.08	0.77	0.77
60	14.95	3.43	1.28	1.04	1.06
75	15.18	4.96	1.96	1.79	2.03
		$\lambda = 1.14\ \mu$, $I_c = 3.9$			
15	1.56	1.34	1.00	0.78	0.72
30	2.86	1.85	1.00	0.67	0.64
45	6.41	2.51	1.05	0.75	0.74
60	14.19	3.26	1.22	0.98	1.01
75	13.41	4.38	1.73	1.58	1.80
		$\lambda = 1.24\ \mu$, $I_c = 4.4$			
15	1.56	1.34	1.00	0.78	0.72
30	2.91	1.88	1.02	0.68	0.65
45	6.68	2.61	1.09	0.78	0.78
60	15.14	3.48	1.30	1.05	1.07
75	16.03	5.24	2.07	1.89	2.15
		$\lambda = 1.31\ \mu$, $I_c = 0.7$			
15	1.57	1.35	1.01	0.78	0.72
30	2.80	1.81	0.98	0.66	0.63
45	5.99	2.34	0.98	0.70	0.70
60	12.53	2.88	1.08	0.87	0.89
75	10.03	3.28	1.30	1.18	1.34
		$\lambda = 1.44\ \mu$, $I_c = 0.5$			
15	1.57	1.35	1.01	0.78	0.72
30	2.86	1.85	1.00	0.67	0.64
45	6.10	2.38	1.00	0.71	0.71
60	12.81	2.94	1.10	0.89	0.91
75	10.24	3.34	1.32	1.21	1.37
		$\lambda = 1.51\ \mu$, $I_c = 0.4$			
15	1.47	1.26	0.94	0.73	0.67
30	2.75	1.78	0.97	0.65	0.62
45	5.95	2.33	0.97	0.70	0.69
60	13.08	3.00	1.12	0.91	0.93
75	11.61	3.79	1.50	1.37	1.56

Table 7 (Continued)

ϑ \ φ	0	45	90	136	180
		$\lambda = 1.53\ \mu$, $I_c = 0.4$			
15	1.57	1.35	1.01	0.78	0.72
30	2.94	1.90	1.03	0.69	0.66
45	6.10	2.38	1.00	0.71	0.71
60	13.42	3.08	1.15	0.93	0.95
75	9.29	3.03	1.20	1.10	1.24
		$\lambda = 1.60\ \mu$, $I_c = 1.5$			
15	1.57	1.35	1.01	0.78	0.79
30	2.90	1.88	1.02	0.68	0.65
45	6.70	2.62	1.09	0.78	0.78
60	15.11	3.47	1.30	1.05	1.07
75	16.42	5.36	2.12	1.94	2.20
		$\lambda = 1.68\ \mu$, $I_c = 1.9$			
15	1.57	1.35	1.01	0.78	0.72
30	2.94	1.90	1.03	0.69	0.66
45	6.70	2.62	1.09	0.78	0.78
60	15.48	3.55	1.33	1.07	1.10
75	16.76	5.47	2.16	1.98	2.24
		$\lambda = 1.81\ \mu$, $I_c = 0.3$			
15	1.55	1.33	0.99	0.77	0.71
30	2.86	1.85	1.00	0.67	0.64
45	6.42	2.51	1.05	0.75	0.75
60	13.68	3.14	1.18	0.95	0.97
75	12.46	4.07	1.61	1.47	1.67
		$\lambda = 1.98\ \mu$, $I_c = 0.1$			
15	1.51	1.30	0.97	0.75	0.69
30	2.71	1.75	0.95	0.64	0.61
45	5.75	2.25	0.94	0.67	0.67
60	12.39	2.84	1.06	0.86	0.88
75	10.72	3.50	1.38	1.26	1.44
		$\lambda = 2.09\ \mu$, $I_c = 0.4$			
15	1.57	1.35	1.01	0.78	0.72
30	2.94	1.90	1.03	0.69	0.66
45	6.24	2.44	1.02	0.73	0.72
60	14.77	3.39	1.27	1.02	1.05
75	15.48	5.06	2.00	1.83	2.07

Table 7 (Continued)

/64

ϑ \ φ	0	45	90	135	180
		$\lambda = 2.19\ \mu$, $I_c = 0.4$			
15	1.57	1.35	1.01	0.78	0.72
30	2.94	1.90	1.03	0.69	0.66
45	6.66	2.60	1.09	0.78	0.77
60	15.27	3.50	1.31	1.06	1.08
75	16.83	5.50	2.17	1.99	2.26
		$z = 0$, $m = 6$			
		$\lambda = 0.72$, $I_c = 8.4$			
15	1.39	1.24	1.02	0.92	0.91
30	2.27	1.74	1.11	0.99	1.00
45	4.31	2.53	1.29	1.18	1.25
60	10.76	3.96	1.65	1.60	1.89
75	31.24	6.54	2.48	2.59	3.46
		$\lambda = 0.76\ \mu$, $I_c = 8.3$			
15	1.40	1.24	1.03	0.92	0.91
30	2.28	1.75	1.12	1.00	1.00
45	4.37	2.57	1.31	1.20	1.27
60	11.08	4.08	1.70	1.64	1.94
75	31.64	6.63	2.51	2.62	3.51
		$\lambda = 0.82\ \mu$, $I_c = 6.0$			
15	1.40	1.24	1.03	0.92	0.91
30	2.28	1.75	1.12	1.00	1.00
45	4.35	2.56	1.30	1.19	1.26
60	10.93	4.03	1.68	1.62	1.92
75	32.67	6.84	2.59	2.71	3.62
		$\lambda = 0.85\ \mu$, $I_c = 5.9$			
15	1.40	1.24	1.03	0.92	0.91
30	2.29	1.76	1.12	1.00	1.00
45	4.38	2.57	1.31	1.20	1.27
60	11.22	4.13	1.72	1.66	1.97
75	35.13	7.36	2.78	2.91	3.90
		$\lambda = 0.93\ \mu$, $I_c = 3.3$			
15	1.39	1.24	1.02	0.92	0.91
30	2.26	1.74	1.11	0.99	0.99
45	4.26	2.51	1.27	1.17	1.24
60	10.55	3.89	1.62	1.57	1.85
75	28.82	6.04	2.28	2.39	3.20

Table 7 (Continued)

/65

ϑ \ φ	0	45	90	135	180
		$\lambda = 1.01\ \mu$, $I_c = 4.0$			
15	1.40	1.25	1.03	0.92	0.92
30	2.29	1.76	1.12	1.00	1.00
45	4.44	2.61	1.33	1.21	1.29
60	11.37	4.19	1.75	1.69	2.00
75	36.34	7.61	2.88	3.01	4.03
		$\lambda = 1.14\ \mu$, $I_c = 1.8$			
15	1.39	1.24	1.02	0.92	0.91
30	2.25	1.73	1.10	0.99	0.99
45	4.30	2.53	1.28	1.18	1.25
60	10.69	3.94	1.64	1.59	1.88
75	31.60	6.62	2.50	2.62	3.50
		$\lambda = 1.24\ \mu$, $I_c = 2.3$			
15	1.39	1.24	1.02	0.92	0.91
30	2.29	1.76	1.12	1.00	1.01
45	4.47	2.63	1.34	1.22	1.30
60	11.51	4.24	1.77	1.71	2.02
75	38.89	8.15	3.08	3.22	4.31
		$\lambda = 1.31\ \mu$, $I_c = 0.29$			
15	1.37	1.22	1.00	0.90	0.89
30	2.26	1.74	1.11	0.99	0.99
45	3.92	2.31	1.17	1.07	1.14
60	9.46	3.49	1.45	1.40	1.66
75	24.35	5.10	1.93	2.02	2.70
		$\lambda = 1.44\ \mu$, $I_c = 0.19$			
15	1.40	1.25	1.03	0.92	0.92
30	2.22	1.71	1.09	0.97	0.98
45	3.91	2.30	1.17	1.07	1.14
60	9.01	3.32	1.38	1.34	1.58
75	21.93	4.59	1.74	1.82	2.43
		$\lambda = 1.51\ \mu$, $I_c = 0.14$			
15	1	1.25	1.03	0.92	0.92
30	2	1.78	1.14	1.01	1.02
45	4.56	2.68	1.36	1.25	1.32
60	12.26	4.52	1.88	1.82	2.15
75	24.88	5.21	1.97	2.06	2.76

Table 7 (Continued)

/66

φ \ ψ	0	45	90	135	180
		$\lambda = 1.53\ \mu$, $I_c = 0.09$			
15	1.40	1.25	1.03	0.92	0.92
30	2.32	1.78	1.14	1.01	1.02
45	4.56	2.68	1.36	1.25	1.32
60	12.26	4.52	1.88	1.82	2.15
75	22.38	4.69	1.77	1.85	2.48
		$\lambda = 1.60\ \mu$, $I_c = 0.82$			
15	1.40	1.25	1.03	0.92	0.92
30	2.31	1.77	1.13	1.01	1.01
45	4.48	2.63	1.34	1.22	1.30
60	11.70	4.31	1.80	1.74	2.06
75	39.56	8.29	3.14	3.28	4.39
		$\lambda = 1.68\ \mu$, $I_c = 1.07$			
15	1.40	1.25	1.03	0.92	0.92
30	2.31	1.77	1.13	1.01	1.01
45	4.48	2.63	1.34	1.22	1.30
60	11.70	4.31	1.80	1.74	2.06
75	39.56	8.29	3.14	3.28	4.39
		$\lambda = 1.81\ \mu$, $I_c = 0.11$			
15	1.37	1.22	1.01	0.91	0.90
30	2.27	1.75	1.11	0.99	1.00
45	4.30	2.53	1.28	1.18	1.25
60	10.17	3.75	1.56	1.51	1.79
75	31.24	6.54	2.48	2.59	3.46
		$\lambda = 1.98\ \mu$, $I_c = 0.05$			
15	1.40	1.25	1.03	0.92	0.92
30	2.32	1.78	1.14	1.01	1.02
45	3.99	2.35	1.19	1.09	1.16
60	9.95	3.67	1.53	1.48	1.75
75	25.15	5.27	1.99	2.08	2.79
		$\lambda = 2.09\ \mu$, $I_c = 0.21$			
15	1.40	1.25	1.03	0.92	0.92
30	2.32	1.78	1.14	1.01	1.02
45	4.45	2.62	1.33	1.22	1.30
60	11.70	4.31	1.80	1.74	2.06
75	39.78	8.34	3.15	3.30	4.46

Table 7 (Continued)

/67

ϑ \ φ	0	45	90	135	180
		$\lambda = 2.19\ \mu$, $I_c = 0.25$			
15	1.40	1.25	1.03	0.92	0.92
30	2.32	1.78	1.14	1.01	1.02
45	4.45	2.62	1.33	1.22	1.30
60	11.70	4.31	1.80	1.74	2.06
75	40.19	8.42	3.18	3.33	4.46
		$z = 3$ км, $m = 2$			
		$\lambda = 0.72\ \mu$, $I_c = 8.5$			
15	1.56	1.34	1.00	0.78	0.72
30	2.91	1.88	1.02	0.68	0.65
45	6.66	2.61	1.09	0.78	0.77
60	15.45	3.54	1.33	1.07	1.10
75	16.46	5.38	2.12	1.94	2.20
		$\lambda = 0.76\ \mu$, $I_c = 6.9$			
15	1.57	1.35	1.01	0.78	0.72
30	2.94	1.90	1.03	0.69	0.66
45	6.71	2.62	1.10	0.79	0.78
60	15.69	3.60	1.35	1.09	1.11
75	17.11	5.59	2.21	2.02	2.29
		$\lambda = 0.82\ \mu$, $I_c = 5.1$			
15	1.57	1.35	1.01	0.78	0.72
30	2.92	1.89	1.02	0.68	0.66
45	6.70	2.62	1.10	0.78	0.78
60	15.87	3.64	1.36	1.10	1.13
75	16.85	5.50	2.18	1.99	2.26
		$\lambda = 0.85\ \mu$, $I_c = 4.3$			
15	1.57	1.35	1.01	0.78	0.72
30	2.94	1.90	1.03	0.69	0.66
45	6.74	2.64	1.10	0.79	0.78
60	15.87	3.64	1.36	1.10	1.13
75	17.28	5.64	2.23	2.04	2.32
		$\lambda = 0.93\ \mu$, $I_c = 3.2$			
15	1.57	1.35	1.01	0.78	0.72
30	2.92	1.89	1.02	0.69	0.66
45	6.66	2.61	1.09	0.78	0.77
60	15.32	3.52	1.32	1.06	1.09
75	16.48	5.38	2.13	1.94	2.21

Table 7 (Continued)

/68

φ \ ϑ	0	45	90	135	180
		$\lambda = 1.01\ \mu$, $I_c = 2.7$			
15	1.57	1.35	1.01	0.78	0.72
30	2.94	1.90	1.03	0.69	0.66
45	6.70	2.62	1.10	0.78	0.78
60	15.68	3.60	1.35	1.09	1.11
75	17.57	5.74	2.27	2.07	2.36
		$\lambda = 1.14\ \mu$, $I_c = 1.7$			
15	1.57	1.34	1.00	0.78	0.72
30	2.92	1.89	1.02	0.68	0.66
45	6.66	2.60	1.09	0.78	0.77
60	15.32	3.52	1.32	1.06	1.09
75	16.42	5.36	2.12	1.94	2.20
		$\lambda = 1.24\ \mu$, $I_c = 1.5$			
15	1.57	1.35	1.01	0.78	0.72
30	2.94	1.90	1.03	0.69	0.66
45	6.80	2.66	1.11	0.80	0.79
60	15.69	3.60	1.35	1.09	1.11
75	17.63	5.76	2.28	2.08	2.36
		$\lambda = 13.1\ \mu$, $I_c = 0.50$			
15	1.54	1.32	0.98	0.76	0.70
30	2.87	1.86	1.01	0.67	0.64
45	6.34	2.48	1.04	0.74	0.74
60	13.55	3.11	1.16	0.94	0.96
75	12.87	4.20	1.66	1.52	1.72
		$\lambda = 1.44\ \mu$, $I_c = 0.33$			
15	1.57	1.35	1.01	0.78	0.72
30	2.88	1.86	1.01	0.68	0.65
45	6.30	2.46	1.03	0.74	0.73
60	13.73	3.15	1.18	0.95	0.97
75	13.08	4.27	1.69	1.54	1.75
		$\lambda = 1.51\ \mu$, $I_c = 0.30$			
15	1.57	1.35	1.01	0.78	0.72
30	2.94	1.90	1.03	0.69	0.66
45	6.24	2.44	1.02	0.73	0.72
60	13.42	3.08	1.15	0.93	0.95
75	10.83	3.54	1.40	1.28	1.45

Table 7 (Continued)

/69

ϑ \ φ	0	45	90	135	180
		$\lambda = 1.53\ \mu$, $I_c = 0.30$			
15	1.57	1.35	1.01	0.78	0.72
30	2.94	1.90	1.03	0.69	0.66
45	6.80	2.66	1.11	0.80	0.79
60	12.08	2.77	1.34	0.84	0.86
75	13.93	4.55	1.80	1.64	1.87
		$\lambda = 1.60\ \mu$, $I_c = 0.48$			
15	1.57	1.35	1.01	0.78	0.72
30	2.94	1.90	1.03	0.69	0.66
45	6.72	2.63	1.10	0.79	0.78
60	15.92	3.65	1.37	1.10	1.13
75	17.91	5.85	2.31	2.11	2.40
		$\lambda = 1.68\ \mu$, $I_c = 0.60$			
15	1.57	1.35	1.01	0.78	0.72
30	2.94	1.90	1.03	0.69	0.66
45	6.80	2.66	1.11	0.80	0.79
60	16.11	3.70	1.38	1.12	1.14
75	18.58	6.07	2.40	2.19	2.49
		$\lambda = 1.81\ \mu$, $I_c = 0.12$			
15	1.57	1.35	1.01	0.78	0.72
30	2.94	1.90	1.03	0.69	0.66
45	6.80	2.66	1.11	0.80	0.79
60	14.37	3.30	1.24	1.00	1.02
75	14.56	4.76	1.88	1.72	1.95
		$\lambda = 1.98\ \mu$, $I_c = 0.06$			
15	1.57	1.35	1.01	0.78	0.72
30	2.94	1.90	1.03	0.69	0.66
45	6.80	2.66	1.11	0.80	0.79
60	14.87	3.41	1.28	1.03	1.06
75	14.29	4.67	1.84	1.69	1.91
		$\lambda = 2.09\ \mu$, $I_c = 0.11$			
15	1.57	1.35	1.01	0.78	0.72
30	2.94	1.90	1.03	0.69	0.66
45	6.80	2.66	1.11	0.80	0.79
60	16.11	3.70	1.38	1.12	1.14
75	18.58	6.07	2.40	2.19	2.49

Table 7 (Continued)

/70

φ / ϑ	0	45	90	135	180
		$\lambda = 2.19\ \mu$, $I_c = 0.11$			
15	1.57	1.35	1.01	0.78	0.72
30	2.94	1.90	1.03	0.69	0.66
45	6.80	2.66	1.11	0.80	0.79
60	16.11	3.70	1.38	1.12	1.14
75	18.58	6.07	2.40	2.19	2.49

References

1. Shifrin, K. S. and Avaste, O. Issledovaniya po fizike atmosfery (Research in the Physics of the Atmosphere), IFA AN ESSR, No. 2, 23, 1960.
2. Johnson, F. S. Journ. Meteorol., 11, 431, 1954.
3. Yamamoto, G. Sci. Rep. Tokyo Univ., Ser. 5, 1, No. 2, 76, 1949.
4. Shifrin, K. S. and Minin, I. N. Trudy GGO, Issue 68, 5, 1957.
5. Kastrov, V. G. Trudy TsAO, Issue 6, 102, 1952.
6. Dave, J. V. and Sekera, Z. Journ. Meteorol., 16, 211, 1959.
7. Prokof'yev, I. A. Atmosfernyy ozone (Atmospheric Ozone), Izd-vo AN SSSR, Moscow-Leningrad, 1951.
8. Howard, J. N., Burch, D. E. and Williams, D. Journ. Am. Opt. Soc., 46, 186, 237, 334, 452, 1956; Geophysical Research Papers No. 40, Nov. 1955, (AF CRC-TR-55-213).
9. Fowle, F. E. Smithsonian Misc. Collect., 68, No. 8, 1917.
10. Kastrov, V. G. Trudy TsAO, Issue 25, 72, 1959.
11. Biryukova, L. A. Trudy TsAO, Issue 25, 72, 1959.
12. Sobolev, V. V. Astronomicheskiy Zhurnal, 20, Nos. 5-6, 14, 1943.
13. Avaste, O. A. and Atroshenko, V. S. Izv. AN SSSR, seriya geofiz., No. 3, 507, 1960.
14. Avaste, O. A. Digest of Actinometrics and Atmospheric Optics (Work of the Conference, Leningrad, January 28-February 4, 1959), Gidrometeoizdat, Leningrad, pp. 270-282, 1961.
15. Feygel'son, Ye. M. and Malkevich, M. S. et al. Trudy IFA AN SSSR, No. 1, 1958.
16. Foitzik, L. and Zchaeck, H. Zeits. f. Meteorol., 7, 1, 1953.
17. Avaste, O. A. Trudy GGO, Issue 109, 13, 1961.
18. Dirmhirn, I. Wetter und Leben (Weather and Life), 9, 41, 1957.
19. Ross, Yu. Avaste, O. A. Research in Physics of Atmosphere, IFA AN ESSR, No. 1, 53, 1959.
20. Yanishevskiy, Yu. D. Trudy GGO, Issue 26, 88, 5, 1951.
21. Adel, A. Phys. Rev., 76, 446, 1949.
22. Bennet, H. E., Bennet, J. M. and Nagel, M. R. Journ. Am. Opt. Soc., 50, 100, 1960.
23. Pyaskovskaya-Fesenkova, Ye. V. Study of Light Diffusion in Earth's Atmosphere, Izd-vo AN SSSR, Moscow, 1957.
24. Kastrov, V. G. Trudy TsAO, Issue 32, 84, 1959.
25. Bell, E. E., Eisner, L., Young, J. and Oetjen, R. A. Journ. Am. Opt. Soc., 50, 1313, 1960.

Translated for the National Aeronautics and Space Administration by John F. Holman and Co. Inc.